A Continuum Model for Elastic Waves in Embedded Carbon Nanotube Composites

BY

Elaf Naeem Mahrous

A Thesis Presented to the

DEANSHIP OF GRADUATE STUDIES

KING FAHD UNIVERSITY OF PETROLEUM & MINERALS

DHAHRAN, SAUDI ARABIA

In Partial Fulfillment of the

Requirements for the Degree of

MASTER OF SCIENCE

In

MECHANICAL ENGINEERING

June 2009

KING FAHD UNIVERSITY OF PETROLEUM & MINERALS

DHAHRAN 31261, SAUDI ARABIA

DEANSHIP OF GRADUATE STUDIES

This thesis, written by **Elaf Naeem Shaker Mahrous** under the direction of his theses advisor and approved by his theses committee, has been presented to and accepted by the Dean of Graduate Studies, in partial fulfillment of the requirements for the degree of **MASTER OF SCIENCE IN MECHANICAL ENGINEERING**.

Thesis Committee

M. Hawwa

Dr. Muhammad Hawwa
(Thesis Advisor)

Dr. Amro Al-Qutub
(Department Chairman)

Dr. Numan Abu-Dheir
(Member)

H-Qahtani

Dr. Salam Zummo
(Dean of Graduate Studies)

Dr. Husien Al Qahtani
(Member)

Date

This work is dedicated to all of my

parents, fiancé, brothers, and sisters

ACKNOWLEDGMENT

It is with great pleasure that I acknowledge the help of many people who assisted me in the preparation and the accomplishment of this work, especially my supportive advisor in KFUPM Dr. **Muhammad Hawwa**.

First of all, strongly I want to thank my **parents and future wife, brothers and sisters** for their sacrifices without which this work could have been completed without insertions.

I would like to express my indebtedness and heartfelt gratitude and appreciation Dr. **Numan Abu-Dheir** and **Husien Al Qahtani** for their precious and constant help and very knowledgeable assistance in supplying creative and helpful advice and in making numerous suggestions for this work. I also wish to thank the other members of my thesis committee for their help and encouragement during this study.

Finally, I appreciate the help of my friends, in ahead of them Mohammed Ali Al Shehri, Basel and Ahmed Qutb Al-Deen, who shared their experiences, ideas and views and helped enrich this work, and to all those who in one way or another contributed to its success.

Acknowledgment is due to the King Fahad University of Petroleum and Minerals for supporting this research.

TABLE OF CONTENT

LIST OF FIGURS

THESIS ABSTRACT

NAME: *Elaf Naeem Mahrous*

Title: ***A Continuum Model for Elastic Waves in Embedded Carbon Nanotube Composites***

Field: ***Mechanical Engineering***

Date: ***June 2009***

The theory of studying the Carbon nanotube (CNT) technology was first introduced in 1991 and it is still under researches and developments. The significance of the Carbon nanotubes (CNTs) is that, their amazing strength, conductivities, and the various ways in which their molecules can be formed and arranged. Therefore, Carbon nanotubes are becoming very important components in the following many fields and applications such as oscillators, charge detectors, clocks, emission devices, sensors, and composites.

The aim of this thesis work is to develop a model for CNT reinforced composite structure based on the continuum approach.

This thesis is explaining in detailed the full procedure of getting the wave model for the CNTs using the averaging method for embedded CNT mixture composites. This procedure included the subsequent steps. First of all is finding the two cylindrical coordinate momentum equations in addition to the constitutive relations for each component in the composite. Then, assessing the symmetry conditions, and evaluating the continuity of the stresses, shears, and deformations around the composite radius. After that, averaging the momentum equations and deriving the relevant partial differential equations that describe the system in terms of the interactions term (ζ and S) and axial displacements (u), which also acquires finding the radial dependence of the shear stress and the radial displacement. Followed by applying the interface

continuity and symmetry conditions for the stresses again along the composites in order to eliminate the stress and get the strains relations along the composites. Subsequently, this will lead to the final equations that describe the composite behavior.

ملخص الرسالة

الاسم: ايلاف بن نعيم بن شاكر محروس

عنوان الرسالة: استخدام نموذج النظرية الاستمرارية لدراسة الموجات المرنة في مركبات أنابيب الكربون النانومترية

التخصص: الهندسة الميكانيكية

تاريخ الدرجة: جمادي الاخرة 1430 هجري (الموافق يونيو 2009 ميلادي)

تكنولوجيا أنابيب الكربون النانومترية اشتهرت مؤخرا في عام 1991م ولا تزال الابحاث مستمرة لاكتشاف مزايا هذه العناصر من حيث قوة الاجهاد والمقاومة و الاستطالة بالاضافة الى مزاياها الحرارية المذهلة. نظرا لهذه المزايا الميكانيكية و الحرارية المذهلة التي تمتلكها أنابيب الكربون النانومترية فانها تستخدم في عدة مجالات هندسية والتي من اهمها مجال مركبات المواد.

ان الهدف من هذه الدراسة المروية هو تطوير استخدام نموذج النظرية الاستمرارية لدراسة الموجات المرنة في مركبات أنابيب الكربون النانومترية المكونة من ثلاث طبقات وذلك من خلال استخدام نظرية حساب متوسط مساحات كل من طبقات المركب. ان نظرية هذه الرسالة تحتوي على الخطوات التالية:

أولا: ايجاد معادلات زخم الحركة بالاضافة الى ايجاد المعادلات الميكانيكية الاساسية لكل من انابيب المركب.

ثانيا: تقييم حالات التناظر والاستمرارية لكل من الاجهاد وجز الاجهاد والاستطالة.

ثالثا: استخدام نظرية حساب متوسط مساحات لكل من طبقات المركب وذلك من خلال تحليل معادلات زخم الحركة والمعادلات الميكانيكية الاساسية ومن ثم ايجاد معادلات التفاضل التي تصف استمرارية كل من انابيب ذلك المركب.

رابعا: استخدام كل من الاستمرارية والتماثل في كل من الانابيب الاسطوانية لحذف الاجهادات ومن ثم استنتاج معادلات الاستطالة في المركب.

وبالتالي ستقودنا هذه الدراسة الى استنتاج المعادلة النهائية التي تصف ميكانيكية الموجات المرنة في مركبات أنابيب الكربون النانومترية المكونة من ثلاث طبقات.

MONENCLATURE

Cnt	*Carbon nanotube*
r	*Radius along the composite*
f	*Filling material inside the composite*
c	*Carbon nanotube inside the composite*
m	*Composite matrix*
σ_{ij}	*Stress tensor*
$\bar{\sigma}_{ij}$	*Averaged stress tensor*
u	*Longitudinal displacement*
$\bar{u}$	*Averaged longitudinal displacement*
v	*Radial displacement*
$\bar{v}$	*Averaged radial displacement*
n_f	*Volume fractions of the composite filling*
n_c	*Volume fractions of the CNT*
n_m	*Volume fractions of the composite matrix*
ζ	*Momentum relation interaction along the composite*
S	*Constitutive relation interaction along the composite*
v^*	*Radial displacement at composite interfaces*
u^*	*Longitudinal displacement at composite interfaces*
$\sigma_{rz}{}^*$	*Shear stress at composites interfaces*

CHAPTER I

INTRODUCTION

This chapter illustrates the motivation behind this thesis, clarifies the problem definition for this thesis, and finally elucidates the thesis outlines.

I.1 MOTIVATION

Carbon nanotubes (CNTs) have amazing properties that no other element has in term of mechanical, chemical, electrical and thermal properties. CNT is the strongest element found until this moment. The fast growth of the industry needs such materials that are reliable and efficient at high operating conditions and experiencing heavy loads. CNTs are used in many engineering composites and also have been applied in many devices, such as atomic-force microscope, field emitters, nanofillers for composite materials, nanoscale electronic devices, and frictionless nanoactuators, nanomotors, nanobearings, and nanospring. Superior mechanical strength of carbon the nanotubes makes them almost ideal force sensor in scanning probe microscopy (SPM) application with having higher durability and ability to image the surfaces with very accurate lateral resolution.

Many studies have been done to study the behavior of the CNTS and their composites. However, those studies are limited to two layer composites.

This thesis will concentrate on a new field of the CNTS composites. It is going to study and advance the composites of the nanotechnology in general and carbon nanotube technology in specific in order to get the ultimate required strength. This will add new and more efficient ways of producing engineering composites that can be used in various engineering applications, to ensure quality of productions and reduce maintenance costs as well.

I.2 PROBLEM DEFINITION

For a CNT reinforced composite, an averaging approach will be used to solve the problem of the wave motion along the fiber's direction. The problem to be studied in this work can be stated as follows:

Based on the continuum approach, develop a wave propagating model for a composite in which CNTs ac as fibers surrounded by a matrix

Thesis is going to evaluate the dynamics, the stresses and strains of the CNTs. Then it will obtain dispersion curves for the CNT reinforced composites.

I.3 THESIS OUTLINE

Chapter 1 is about the general introduction to the thesis. Chapter 2 contains the general definition of the nanotechnology and the aspects and properties of the CNTs. Chapter 3 includes the modeling types of the CNTS, which are the molecular dynamics model and continuum model. Chapter 4 discusses the averaging model principles, advantages, and to prove that averaging model is extremely appropriate for the CNTs composites. Chapter 5 explains how to form and solve the wave continuum model for the CNTS composites. Chapter 6 discusses the final results of the developed continuum mixture model in embedded CNTs composites. This thesis is ended with chapter 7 containing research conclusions and recommendations for using the thesis proposed model.

CHAPTER II

NANOTECHNOLOGY AND CARBON NANOTUBES

This Chapter will define the nanotechnology in general and the carbon nanotube in detailed. It will also identify the carbon nanotube discovery, properties and applications.

II.1 DEFINITION OF NANOTECHNOLOGY

The term "nanotechnology" was first defined in 1974 by Tokyo Science University Professor Norio Taniguchi paper as follows: "Nano-technology" mainly consists of the processing of, separation, consolidation, and deformation of materials by one atom or by one molecule "[1]. Actually, the basic idea of this definition is now expanded and explored in much more depth and details such that; it is the technology that involves the construction of useful devices and systems on the nanometer length scale, and also analyze their phenomena and properties (physical, chemical, biological) at that length scale.

II.2 CARBON NANOTUBES ASPECTS

Carbon nanotube (CNT) is one of the most important materials discovered for the time being. This section is an overview of the carbon nanotubes classification, discovery, and amazing carbon nanotubes properties. Furthermore, this chapter illustrates the CNTs types and how these materials are made. Finally, it briefly gives examples for some of the CNTs applications.

II.2.1 Classification of CNT

Carbon nanotubes are members of the fullerene structural group that also includes Bucky balls. Whereas Bucky balls are spherical in shape, a nanotube is cylindrical, with at least one end typically capped with a hemisphere of the Bucky ball structure. Their name is derived from their size, so that the diameter of a carbon nanotube is on the order of a few nanometers (approximately 50,000 times smaller than the width of a human hair), while they can be up to several millimeters in length. [2]

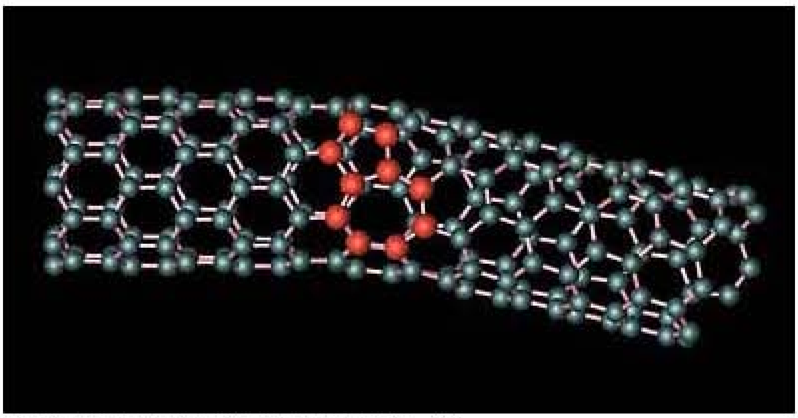

Figure 1: structures of carbon nanotube. [3]

Carbon nanotubes and their reinforced composites are the most promising building blocks in the field of future engineering applications [4]. Actually, CNTs have a very high potential to improve the mechanical properties of the materials [5, 6].

II.2.2 CNTs Discovery

In 1952, Radushkevich and Lukyanovich published clear images of 50 nanometer diameter tubes made of carbon in the Russian Journal of Physical Chemistry. This discovery was unnoticed because the article was published in the Russian language, and Western scientists' access to Russian press was limited during the Cold War. It is most likely that carbon nanotubes were discovered before this date, but the invention of the transmission electron microscope allowed the direct visualization of these structures [7].

After the CNTs discovery, scientists have realized that the theoretically calculated mechanical properties of these attractive structures such as high stiffness, low density, high strength and structural perfection could make them idealistic for a wealth of technological revolution. However, the experimental confirmation and refutation of these predictions and by using the most advanced computer programs and simulations have complicated the issue and showed that the carbon nanotube is really a huge area of technology that needs further investigations and development.

II.2.3 Strength and Thermal Properties of CNTs

Carbon Nanotubes have incredible amazing properties. This section illustrates the CNTs strength and thermal properties.

II.2.3.1 CNTs Strength

CNTs have been found to have the highest elastic modulus among all the materials in nature with Young's modulus greater that one TPa [8, 9]. So, carbon nanotubes are one of the strongest materials known, both in terms of tensile strength and elastic modulus. This strength results from the covalent sp^2 bonds formed between the individual carbon atoms. In comparison, high-carbon steel has a tensile strength that is approximately 1.2 GPa. Since carbon nanotubes have a low density for a solid of 1.3-1.4 g/cm^3, its specific strength is the best of known materials [10]. Moreover, in adding the CNTs to the polymers, the elastic modulus of the polymer is seen to rise by addition of CNTs [11]. Amazingly, by adding only 1.0 % of CNTs can increase the elastic modulus for some of the polymer by 100% [12]. Also, it has been found that CNTs prevent crack propagation by bridging them [13, 14].

For the carbon nanotubes ceramic composites, unfortunately, it has been proven that carbon nanotubes don't affect the ceramic materials strength or toughness as expected. The main reason of that is the weak bonding coherent between the composite surfaces. However, this problem was fortunately solved by using acid treatments and the combination of the adherent with a mechanical interlock induced by the chemically modified CNTs. Many experiments had been implemented to solve these ceramic CNTs bonding problems, and the mechanical results and measurements reveal that by adding only 0.9 volume % acid treated CNT addition can results in 27% and 25 % increase in bending strength and fracture toughness, respectively. [15]

Under excessive tensile strain, the tubes will undergo plastic deformation, which means the deformation is permanent. This deformation begins at strains of approximately 5% and can increase the maximum strain the tube undergoes before fracture by releasing strain energy. [10]

CNTs are not however, as strong under compression. They are weaker because of their hollow structure and high aspect ratio, so that they tend to undergo buckling when placed under compressive, tensional or bending stresses [16].

II.2.3.2 CNT Thermal Properties

Carbon nanotubes are found to be excellent thermal conductors along the tube, exhibiting a property known as "ballistic conduction," but also it is a good insulator laterally to the tube axis. The carbon nanotubes are also found to be able to transmit up to 6000 watts per meter per Kelvin at room temperature. Moreover, the temperature stability of carbon nanotubes is expected to be up to about 750 degrees Celsius in air and 2800 degrees Celsius in vacuum. [17]

II.2.4 Single-Walled Carbon Nanotubes

One of the main types of carbon nanotube is the single-walled carbon nanotubes (SWNTs).

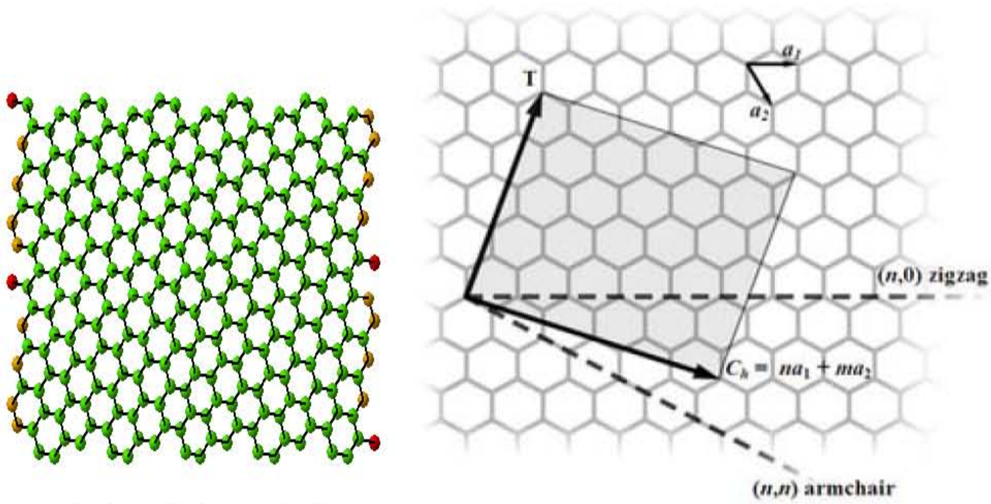

Figure 2, single-walled CNT. [18]

The structure of a SWNT, as shown in figure (2), can be conceptualized by wrapping a one-atom-thick layer of graphite called graphene into a seamless cylinder. The (n,m) nanotube naming scheme can be thought of as a vector (C_h) in an infinite graphene sheet that describes how to "roll up" the graphene sheet to make the nanotube. T denotes the tube axis, and $\mathbf{a}_1$ and $\mathbf{a}_2$ are the unit vectors of graphene in real space.

Most single-walled nanotubes (SWNT) have a diameter of close to 1 nanometer, with a tube length that can be many thousands of times larger. Single-walled nanotubes with length up to orders of centimeters have been produced. The way the graphene sheet is wrapped is represented by a pair of indices (n,m) called the chiral vector. The integers n and m denote the number of unit vectors along two directions in the honeycomb crystal lattice of graphene. If m=0, the nanotubes are called "zigzag". If n=m, the nanotubes are called "armchair". If n≠m, the nanotubes are "helical"[19]

Mainly, as shown in Figure (3), there are three types of SWCNTs structures which are:

(a) A zig-zag type nanotube,

(b) An armchair type nanotube,

(c) A helical nanotube.

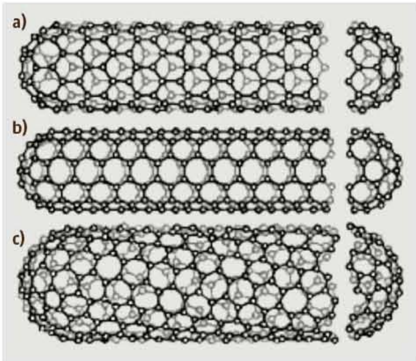

Fig. 3, Sketch of three different SWNT structures as examples for (a) a zig-zag-type nanotube, (b) an armchair type nanotube, (c) a helical nanotube. [19]

II.2.5 Processing of CNTs Materials

There are many methods and techniques for producing the carbon nanotube composites. An important and one of the first developed methods is the synthesis method for both single and multi-walled CNTs [20]. The primary synthesis method includes arc-discharge, laser ablation, gas-phase catalytic growth form carbon monoxide, and chemical vapor deposition known as (CVD) [21-24]. Actually, large quantities of nanotubes are needed for the CNTs to get embedded in composites [20]. Therefore, the scale-up limitation of both the arc discharge and the laser ablation techniques would make the cost of the nanotube based composites extensively high [20]. Moreover, impurities in the form of catalyst particles, nanotubular fullerenes, and amorphous carbon are produced during the CNT synthesis [20]. Therefore, a purification step is needed to separate the tubes. Hence, the gas-phase processes tend to turn out nanotubes with fewer impurities and also more amenable to large scale processing.

Iijima [21] observed first the nanotubes synthesized through the electric-arc discharge method which is shown in figure (4) below [20].

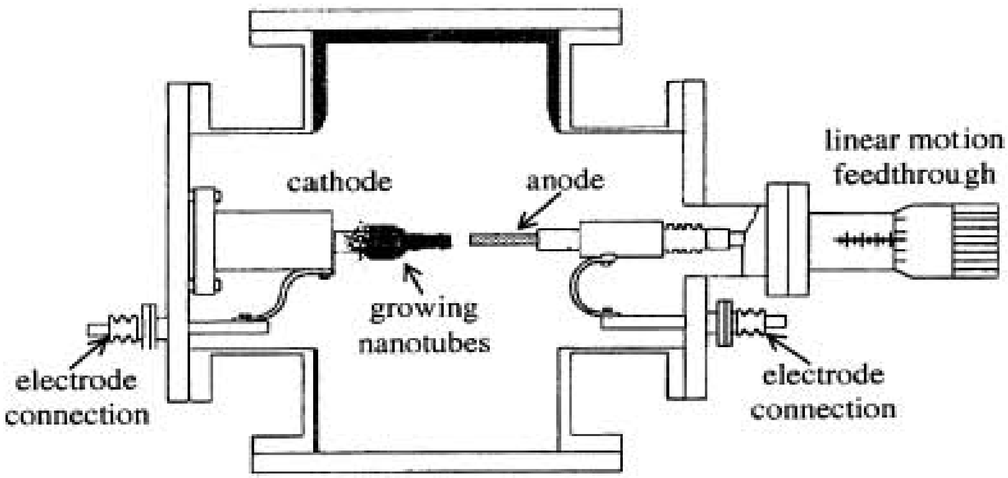

Figure 4: schematic illustration of the arc-discharge technique. [20]

The above figure involves the use of two high purity graphite rods as anode and cathode. These rods are brought under a helium atmosphere and then a voltage is applied until a stable arc is achieved. The accurate process variables depend on the graphite rods. Once the anode is consumed, constant gap between the cathode and anode is maintained by adjusting the anode position. Then, the material deposits on the cathode to form a build-up consisting of an outside shell of fused materials and soft fibrous core nanotues and other carbon particles [25-29].

Laser ablation technique actually was used first for the initial synthesis of fullerenes. Then, this technique has been improved to produce single-walled nanotubes [30]. In this technique, as shown in figure (5), laser is used in order to vaporize a graphite target that is doped with cobalt and nickels catalyst and held in a controlled atmosphere oven at almost 1200 centigrade. Finally, the condensed material is collected on a water cooled target.

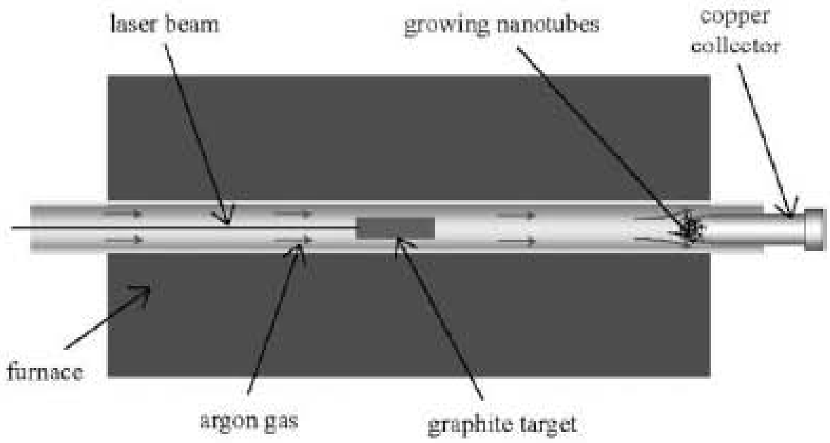

Figure 5: schematic of the laser ablation process. [50]

Unfortunately, the arc-discharge and the laser ablation techniques are limited in the volume of sample that they can produce in relation of the size of the carbon source. Also, purification steps are necessary in order to separate the tubes from the undesirable by products. Subsequently, these limitations have motivated the scientists to develop the gas-phase technique. In this technique, nanotubes are mainly formed by the decomposition of the carbon containing gas. This technique is amenable to continuous processes because the carbon source is continually replaced by flowing gas. Furthermore, the produced nanotubes have high purities if using this method even with less subsequent purification steps. [20]

One unique and important advantage of CVD is the ability to synthesize aligned array of CNTs with controlled length and diameter. Further modification of the synthesis to obtain straight and well aligned CNTs has been accomplished by the use of plasma enhanced chemical vapor deposition (PECVD) in which the plasma is excited by a DC source or a microwave source that improve the chemical reaction which assists in enhancing accuracy of the CNTs parameters and properties. [20]

II.2.6 Applications of CNT

CNTs have been applied in many devices, such as atomic-force microscope, field emitters, nanofillers for composite materials, nanoscale electronic devices, and frictionless nanoactuators, nanomotors, nanobearings, and nanospring. Superior mechanical strength of carbon the nanotubes makes them almost ideal force sensor in scanning probe microscopy (SPM) application with having higher durability and ability to image the surfaces with very accurate lateral resolution.

CHAPTER III

MECHANICAL MODELING OF CNT

The modeling for theoretical analysis is classified into two main categories: These models mainly are the atomic models and the continuum models. This section will discuss both of these models and illustrate the differences between them.

III.1 MOLECULAR DYNAMICS MODEL

In a molecular structure, the bonded and non-bonding interactions of the CNT atoms can be quantitatively described by the molecular mechanics.

These atomic methods are only applicable to systems with a small number of molecules and atoms and therefore restrained only to small-scale modeling.

The bonds forces that result from the relative atomic positions are described by the force field in which these forces contribute to the total molecular potential energy for this nano-structured material [31]. Subsequently, the molecular potential energy for the CNT can be described by the sum of the individual energy contribution in the molecular model. Then, all of the individual energy contributions are summed over the total corresponding interactions numbers in the molecular model [32]. So, the molecular dynamic (MD) model studies the physics of the condensed matter systems in which the forces acting on the nano-sturcture particles in a defined cell are calculated and also the classical Newtonian principles of motions are fully numerically integrated [33-35]. As a matter of fact, these atomic methods are only applicable to systems with a small number of molecules and atoms and therefore restrained only to small-scale modeling [36-38].

III.2 CONTINUUM MECHANICS AND CONTINUUM MODEL

To understand what a continuum mechanics is, this thesis will explain each term independently. Then it will explain the continuum mechanism as one scientific term.
First, it would be more convenient to start with the definition of the "mechanics" definition." Mechanics" is the study of the motion and the forces of the matter. The main meaning and key objective of the mechanics is performing the problem formula and getting the appropriate solution of initial boundary-value problem model as a real physical phenomenon.
Second, the term continuum generally indicates the real line. More generally, continuum is somewhat a linearly ordered set of much more than only one element and can be described as a densely ordered. This means between any two members there is found another. Moreover, continuum denotes the lack of gaps in sense that non-empty subset with explicit boundaries. Therefore, continuum is a nonempty connected space.
In addition to counting for the vicinity within the body, one more important focus in continuum is the existence of nontrivial indecomposable continua [39].

To combine the first and second definitions into a "continuum mechanics", it is well known that matter is created and formed of molecules that in turn consist of atoms and subatomic particles. Therefore, the theory of describing the relationships between gross phenomena and taking in consideration how to deal with the materials on a smaller scale and how to analyze and realize the forces acting on them is known as the continuum mechanics. For example, the diameter of the red blood cell in our body is about 8 μm; so, by the continuum mechanics approach it can be treated as a continuum if it has been considered its flow, motion, movements, forces acting on it, and its responses in arteries of diameter say 0.5 mm [39]. Therefore, the Continuum mechanics is a mental, logical, technical, and an external category imposed by professional engineers and scientist on their observations and on the resulting details. Therefore, it provides and serves as an idealized approximation of the reality and gives a model which is asymptotic to the universe as it is. Moreover, at nanometer scales, spacing between individual atoms is extremely important and the ordinary discrete structure of analyzing the materials properties may lose its homogeneity. Therefore, an averaging continuum model is becoming essential for such analysis and for detailed studies.

Recently, many models have been introduced and applied to estimate and deeply study the mechanical properties of the composites such as the thermo-mechanical properties, young's modulus, and efficiency of the reinforcement. Some of these models are Mori-Tanaka model for calculating the effect of filler aspect ratio and modulus on the longitudinal reinforcement of the composites based on fiber and disk like fillers, zheng model for elastic properties of stationary and flow-induced phases of nano-rod-polymer model, Halpin-Tsai model for analyzing the elastic aspects of the micromechanics of clay based polymer nano-composites. [40]

CHAPTER IV

WAVE MODEL USING THE AVERAGING METHOD

This chapter explains the averaging method theory. After that, identifies the main averaging model advantages. Then, it will elucidate two important issues that need to be clarified before proceeding with the continuum modeling. These issues are the interfacial bonding and the proper dispersion of the individual CNTs inside the matrix.

IV.1 THE AVERAGING METHOD THEORY

The main idea behind the averaging method is to reduce the two dimensional problem to a quasi-one-dimensional one and to define effective unidirectional field quantities. For this proposed improved continuum mixture model, the model is developed for the propagation of axisymmetric longitudinal waves composite. It is achieved by the solving the axial rate of change of the radial displacement in the shear constitutive relations.

Science the continuum mechanics principle in mathematical formula was considering the sum of the particles as:

$$I = \int_a^b f\,(x)\,dx$$

Therefore, the area averaging method of the continuum model is going to come out as:

$$\overline{(\quad)_f} = \frac{1}{\pi\, r^2}\int_0^r f(\quad)_f\,dr$$

IV.2 AVERAGING CONTINUUM MODELS ADVANTAGES

The main advantages of the averaging continuum models are:

1. The averaging continuum model serves as an idealized approximation of the reality and can be very accurate in capturing the dominant periods as well as the time history response for different applications. For example, vibration applications, designing of large lattice structure, and stress and strain applications [41].
2. The averaging continuum model doesn't have to be symmetric, isotropic, or homogenous. Also, it counts the different behaviors between the filler and the matrix inside the nano-composites. [39]
3. Due to the considerable reduction in the computational effort, the continuum method is easier and much attractive for the analysis of large frames and also for the use in preliminary design.
4. Averaging continuum model and principle is applicable all media for both solids and fluids and under all kinds of loading conditions.
5. This continuum model gives growth to the quality, function, derivation, emergence, influence, fields, interactions, processes and measurements concepts in all branches of physics, chemistry, engineering and also biology. [39]

IV.3 INTERFACIAL BONDING OF THE CNTS COMPOSITES

The strong interfacial bonding of the CNTs composites first is important to be guaranteed. Therefore, Wangner and co-workers investigated focusing on the interfacial bonding by performing a pull-out experiments of individual CNTs from a polymer matrix in order to evaluate the interfacial shear strength of the nanotube system [42,43]. Unfortunately, they found that the bonds between the filling materials and the matrix are not perfectly congested. However, scientists fortunately found that an excellent enhancement of the interfacial adhesion can be achieved by adding chemicals adherents inside the composites [4]. Furthermore, Frankland found that the interfacial shear strength would be greatly improved by over an order of magnitude without decreasing the Young's modulus significantly if only one percent of the carbon atoms of the CNT surface are covalently bonded to the matrix [44]. As a result, the full transfer of the stresses can be guaranteed while performing the averaging continuum model [4].

IV.4 DISPERSION OF THE INDIVIDUAL CNTS INSIDE THE MATRIX

The second main problem that is needed to be discussed, clarified, and solved is the dispersion of the CNTs in the matrix system [4]. The nano-scale particles exhibit an enormous surface area that is several orders of magnitude greater than the surface of conventional fillers. This surface area is not only acting as interface for a stress transfer, but also responsible for the strong tendency of the carbon nanotubes to form agglomerates. Therefore, the efficient exploitation of the carbon nanotubes properties in matrices is directly related to their homogenous dispersion in those matrices [4].

Common and most used technique for the dispersion of the CNTs is the sonication technique [4]. In this method, a pulsed ultrasound exfoliates agglomerates and as a result disperses CNTs in the matrix effectively [4]. Unfortunately, this sonication technique is only effective and manageable for small batches due to the high reduction of the vibrational energy results as an increasing distance from the sonic tip [45-47].

Providentially, this dispersion problem was recently solved. The most effective technique that shows an excellent and precise dispersion results and focuses on the improved dispersion of the CNTs in the matrices is the shear-mixing technique which is also known as the calander technique [4]. Lately, Yasmin et al. reported about a very effective and excellent exfoliation and dispersion of the nano-scaled montmorillonite in a DEGBA epoxy resin using three roll calander [48]

.

CHAPTER V

FORMING THE WAVE CONTINUUM MIXTURE MODEL FOR WAVE PROPAGATION IN AN EMBEDDED CNT FIBROUS COMPOSITE

Before developing the continuum mixture model for wave propagation in embedded CNT fibrous composites in this thesis, it is important to enlighten and reemphasis the importance of the continuum theory in general and the averaged continuum model in specific. As a matter of fact, many scientists have used and are still using the continuum models. For example, Robel developed in 1970 a continuum theory of mixtures including electromagnetic and thermodynamic aspects [49]. Also, Hegemier and Nayfeh developed in 1973 a continuum mixture theory for wave propagation in elastic laminated composites [50]. Moreover, Bache also developed in 1974 a continuum theory for wave propagation in laminated [50]. Furthermore, Nayfeh and Gurtmann predicted in 1974 the elastic properties of the cellular materials using the averaged continuum mixture theory [51]. Additionally, continuum mixture theory was also developed by McNiven and Mengi in 1970 in order to predict the elastic properties of cellular materials [51]. Also, a continuum model was developed in 1986 by Roben for the crystals and quasicrystals [52]. Similarly, Jennifer Jingxuan Dong used in 1993 a continuum mixture theory to find the wave propagation in axially polarized piezoelectric fibrous composites [53]. Amazingly, even in the chemistry field the continuum model can be used. For example, a continuum theory of chemically reacting media has been developed in 2005 by Ingram and Eringen [54]. Currently, many scientists are developing and improving the continuum mixture theory for vast numbers of composites for different structures and applications.

Presently, let us start developing this model. The CNT model inside the embedded CNT fibrous composites is assumed as shown:

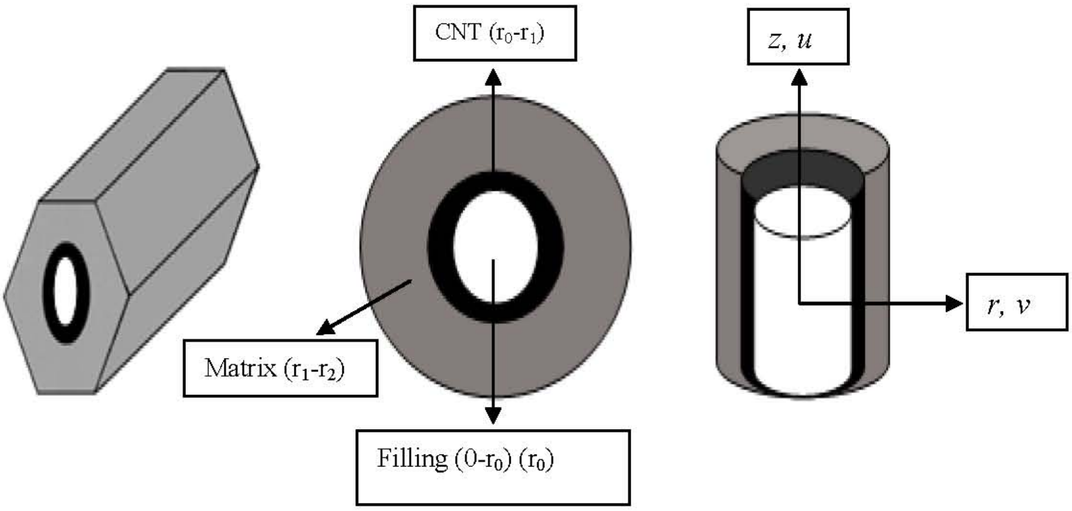

Figure 6: embedded CNT fibrous composite Carbon nanotube composite cylinder model which is found inside the matrix.

We would have r_0, r_1, and r_2 where, the distance from 0 to r_0 is the filling inside the CNT, and from r_0 to r_1 is the CNT, and from r_1 to r_2 is the matrix. The filling in this thesis will be finally assumed as air.

The fillings are made up of an isotropic material and they are uniformly distributed in an isotropic matrix. Also, hexagonal symmetry of the unidirectional reinforced composite can be considered as cylindrical symmetry for simplicity. Due to the cylindrical symmetry, the axial rate of change of the radial displacement for the shear constitutive relation of the composite is neglected. As a result, the two-dimensional field equations that hold in all layers (filling, CNT, and matrix) are reduced to a quasi-one-dimensional system of coupled partial differential equations that satisfy all the radial boundary and interfacial conditions. Then, the harmonic solution for the field variables will be assumed to solve and obtain the final wave propagation solution.

For the axisymmetric longitudinal wave propagation, the composite behavior will be described by the following two cylindrical coordinate momentum equations:

$$\frac{\partial \sigma_z}{\partial z} + \frac{1}{r}\frac{\partial}{\partial z}(r\,\sigma_{rz}) = \rho\,\frac{\partial^2 u}{\partial t^2} \tag{1}$$

$$\frac{\partial \sigma_r}{\partial r} + \frac{\partial \sigma_{rz}}{\partial z} + \frac{1}{r}\,(\sigma_r - \sigma_\theta) = \rho\,\frac{\partial^2 v}{\partial t^2} \tag{2}$$

Identifying the filling, carbon nanotube, and matrix materials with the subscripts f, c, and m, respectively, the filling, CNT and the matrix have isotopic materials constitutive relations of the form:

$$\begin{bmatrix} \sigma_z \\ \sigma_\theta \\ \sigma_r \\ \sigma_{r\theta} \\ \sigma_{rz} \\ \sigma_{\theta z} \end{bmatrix} \begin{matrix} = \\ = \\ = \\ = \\ = \\ = \end{matrix} \begin{bmatrix} f11 & f12 & f12 & 0 & 0 & 0 \\ f12 & f11 & f12 & 0 & 0 & 0 \\ f12 & f12 & f11 & 0 & 0 & 0 \\ 0 & 0 & 0 & f44 & 0 & 0 \\ 0 & 0 & 0 & 0 & f44 & 0 \\ 0 & 0 & 0 & 0 & 0 & f44 \end{bmatrix} \begin{bmatrix} \varepsilon_z \\ \varepsilon_\theta \\ \varepsilon_r \\ \gamma_{r\theta} \\ \gamma_{rz} \\ \gamma_{\theta z} \end{bmatrix} \tag{3}$$

$$\begin{bmatrix} \sigma_z \\ \sigma_\theta \\ \sigma_r \\ \sigma_{r\theta} \\ \sigma_{rz} \\ \sigma_{\theta z} \end{bmatrix} = \begin{bmatrix} c11 & c12 & c12 & 0 & 0 & 0 \\ c12 & c11 & c12 & 0 & 0 & 0 \\ c12 & c12 & c11 & 0 & 0 & 0 \\ 0 & 0 & 0 & c44 & 0 & 0 \\ 0 & 0 & 0 & 0 & c44 & 0 \\ 0 & 0 & 0 & 0 & 0 & c44 \end{bmatrix} \begin{bmatrix} \varepsilon_z \\ \varepsilon_\theta \\ \varepsilon_r \\ \gamma_{r\theta} \\ \gamma_{rz} \\ \gamma_{\theta z} \end{bmatrix} \quad (4)$$

$$\begin{bmatrix} \sigma_z \\ \sigma_\theta \\ \sigma_r \\ \sigma_{r\theta} \\ \sigma_{rz} \\ \sigma_{\theta z} \end{bmatrix} = \begin{bmatrix} m11 & m12 & m12 & 0 & 0 & 0 \\ m12 & m11 & m12 & 0 & 0 & 0 \\ m12 & m12 & m11 & 0 & 0 & 0 \\ 0 & 0 & 0 & m44 & 0 & 0 \\ 0 & 0 & 0 & 0 & m44 & 0 \\ 0 & 0 & 0 & 0 & 0 & m44 \end{bmatrix} \begin{bmatrix} \varepsilon_z \\ \varepsilon_\theta \\ \varepsilon_r \\ \gamma_{r\theta} \\ \gamma_{rz} \\ \gamma_{\theta z} \end{bmatrix} \quad (5)$$

where,

$$\varepsilon_z = \frac{\partial u}{\partial z}, \qquad \varepsilon_r = \frac{\partial v}{\partial r}, \qquad \varepsilon_\theta = \frac{v}{r}, \qquad \gamma_{rz} = \frac{\partial v}{\partial z} + \frac{\partial u}{\partial r} \quad (6)$$

Where σ_{ij} is the stress tensor, u and v are the displacement components in the longitudinal and radial directions, respectively.

Now, after the expansion of the above equations for the use of axisymmetric longitudinal wave propagation in our system, the following constitutive relations for all the fillings, CNT, and matrix are generally generated as:

$$\sigma_z = C_{11} \frac{\partial u}{\partial z} + \frac{C_{12}}{r} \frac{\partial}{\partial r}(r\, v) \tag{7}$$

$$\sigma_r = C_{22} \frac{\partial \nu}{\partial r} + \frac{C_{12}}{r}\, v + C_{12} \frac{\partial u}{\partial z} \tag{8}$$

$$\sigma_\theta = C_{11} \frac{v}{r} + C_{12} \frac{\partial v}{\partial r} + C_{12} \frac{\partial u}{\partial z} \tag{9}$$

$$\sigma_{rz} = C_{44} (\frac{\partial v}{\partial z} + \frac{\partial u}{\partial r}) \tag{10}$$

Where C_{ij}=f_{ij} for the filling, C_{ij}=c_{ij} for the carbon nanotube, and C_{ij}=m_{ij} for the matrix. The above field equations have also the following symmetry and continuity conditions along (*z, r, t*):

$$v_f(z, 0, t) = 0 \tag{11.a}$$

$$\sigma_{rz_f}(z, 0, t) = 0 \tag{11.b}$$

$$\sigma_{rz_m}(z, r_2, t) = 0 \tag{11.c}$$

$$v_m(z, r_2, t) = 0 \tag{11.d}$$

Also, due to the continuity on r = r_0 we will get:

$$\sigma_{rz_f}(z, r_0, t) = \sigma_{rz_c}(z, r_0, t) \tag{11.e}$$

$$\sigma_{r_f}(z, r_0, t) = \sigma_{r_c}(z, r_0, t) \tag{11.f}$$

$$u_f(z, r_0, t) = u_c(z, r_0, t) \tag{11.g}$$

$$v_f(z, r_0, t) = v_c(z, r_0, t) \tag{11.h}$$

In addition, due to the continuity on r = r_1 we will get:

$$\sigma_{rz_c}(z, r_1, t) = \sigma_{rz_m}(z, r_1, t) \tag{11.g}$$

$$\sigma_{r_c}(z, r_1, t) = \sigma_{r_m}(z, r_1, t) \tag{11.h}$$

$$u_c(z, r_1, t) = u_m(z, r_1, t) \tag{11.i}$$

$$v_c(z, r_1, t) = v_m(z, r_1, t) \tag{11.j}$$

V.1 Method of Solution

The Area-Averaging method solution will be used to reach our solution as:

$$\overline{(\quad)_f} = \frac{1}{\pi\, r_0{}^2} \int_0^r 2\pi (\quad)_f \, dr \tag{12.a}$$

$$\overline{(\quad)_c} = \frac{1}{\pi\, (r_1{}^2 - r_0{}^2)} \int_0^r 2\pi\, (\quad)_c \, dr \tag{12.b}$$

$$\overline{(\quad)_m} = \frac{1}{\pi\, (r_2{}^2 - r_1{}^2)} \int_0^r 2\pi\, (\quad)_m \, dr \tag{12.c}$$

Now, by defining n_f, n_c and n_m to be the volume fractions of the fillings, carbon nanotube, and the matrix, respectively, and also ζ and S denote the momentum and the constitutive relations interaction terms respectively as:

$$n_f = \frac{r_0{}^2}{r_2{}^2} \tag{13.a}$$

$$n_c = \frac{(r_1{}^2 - r_0{}^2)}{r_2{}^2} \tag{13.c}$$

$$n_m = \frac{(r_2{}^2 - r_1{}^2)}{r_2{}^2} \tag{13.c}$$

$$\zeta_1 = \frac{2\, n_f \sigma_{rz_1}{}^*}{r_0} \tag{13.d}$$

$$\zeta_2 = \frac{2\,(n_f + n_c)\sigma_{rz\,2}{}^{*}}{r_1} \tag{13.e}$$

$$S_1 = \frac{2\,n_f v_1{}^{*}}{r_0} \tag{13.f}$$

$$S_2 = \frac{2\,(n_f + n_c) v_2{}^{*}}{r_1} \tag{13.g}$$

Where $v_1{}^{*}$,$v_2{}^{*}$,$\sigma_{rz_1}{}^{*}$, and $\sigma_{rz_2}{}^{*}$ are the interface the radial displacement and shear stress at r_0 and r_1 respectively.

So, by integrating equations (1) and (7) and using the symmetry and continuity conditions for equations (11), the following quasi-one-dimensional momentum equations will be obtained as:

First,

From averaging the momentum equation we are going to get:

$$n_f \frac{\partial \overline{\sigma_{z_f}}}{\partial z} = - \frac{2\,n_f\,\sigma_{rz\,1}{}^{*}}{r_0} + n_f\,\rho_f\,\frac{\partial^2 \overline{u_f}}{\partial t^2} \tag{14.a}$$

$$n_f \frac{\partial \overline{\sigma_{z_f}}}{\partial z} = - \zeta_1 + n_f\,\rho_f\,\frac{\partial^2 \overline{u_f}}{\partial t^2} \tag{14.b}$$

Then, from the constitutive relations from (r_0 to r_1):

$$n_c \frac{\partial \overline{\sigma_{z_c}}}{\partial z} + \frac{2\, {\sigma_{rz}}_1{}^{*}\, r_1}{{r_2}^2} - \frac{2\, {\sigma_{rz}}_1{}^{*}\, r_0}{{r_2}^2} = n_c\, \rho_c \frac{\partial^2 \overline{u_c}}{\partial t^2} \qquad (15.a)$$

$$n_c \frac{\partial \overline{\sigma_{zc}}}{\partial z} + \frac{2\,(n_{f+n_c}) {\sigma_{rz}}_2{}^{*}}{r_1} - \frac{2\, n_f {\sigma_{rz}}_1{}^{*}}{r_0} = n_c\, \rho_c \frac{\partial^2 \overline{u_c}}{\partial t^2} \qquad (6.15.b)$$

$$n_c \frac{\partial \overline{\sigma_{zc}}}{\partial z} + \zeta_2 - \zeta_1 = n_c\, \rho_c \frac{\partial^2 \overline{u_c}}{\partial t^2} \qquad (15.c)$$

Finally, from ($r_1\ to\ r_2$):

$$n_m \frac{\partial \overline{\sigma_{zm}}}{\partial z} - \frac{2{\sigma_{rz}}_2{}^{*}\, r_1}{{r_2}^2} = n_m\, \rho_m \frac{\partial^2 \overline{u_c}}{\partial t^2} \qquad (16.a)$$

$$n_m \frac{\partial \overline{\sigma_{zm}}}{\partial z} - \zeta_2 = n_m\, \rho_m \frac{\partial^2 \overline{u_m}}{\partial t^2} \qquad (16.b)$$

Now, using the constitutive equation (7) and by averaging the above relation to get:

First from (0 to r_0)

$$n_f\, \overline{\sigma_{zf}} = f_{12}\, S_1 + n_f\, f_{11} \frac{\partial \overline{u_f}}{\partial z} \qquad (17)$$

Then, from ($r_0\ to\ r_1$)

$$\overline{\sigma_{zc}} = c_{11}\frac{\partial \overline{u_c}}{\partial z} - \frac{2\, c_{12}}{r_0{}^2 - r_1{}^2}\left[r_1 v_2{}^{*} - r_0 v_1{}^{*}\right] \tag{18.a}$$

Multiply by n_c to get:

$$n_c\overline{\sigma_{zc}} = n_c c_{11}\frac{\partial \overline{u_c}}{\partial z} + c_{12}(S_2 - S_1) \tag{18.b}$$

Then, from (r_1 to r_2)

$$\overline{\sigma_{zm}} = \frac{2\, m_{12}}{r_0{}^2 - r_2{}^2} r_1 v_2{}^{*} + m_{11}\frac{\partial \overline{u_m}}{\partial z} \tag{19.a}$$

$$n_m\, \overline{\sigma_{zm}} = -\, m_{12}S_2 + n_m\, m_{11}\frac{\partial \overline{u_m}}{\partial z} \tag{19.b}$$

V.2 Evaluation of ζ and S

To derive the relevant partial differential equations that describe the system in terms of the interactions term (ζ_1, ζ_2, S_1, and S_2) and axial displacements ($\overline{u_f}$, $\overline{u_c}$, and $\overline{u_m}$), the constitutive relations of equations must be used. This will help in reducing the equations (8)-(10) to a quasi-one-dimensional one that retains the integrity of the propagation in the composite. Therefore, this approach concerns with the radial dependence of the shear stress and the radial displacement. Now, from the continuity and symmetry it has been assumed that:

$$v_f(z,r,t) = B_1(z,t)\, r \tag{20.a}$$

$$v_c(z,r,t) = B_1(z,t)\frac{n_f}{n_c}\left(\frac{{r_1}^2}{r^2} - 1\right) r - B_2(z,t)\frac{(1-n_m)}{n_c}\left(\frac{{r_0}^2}{r^2} - 1\right) r \tag{20.b}$$

$$v_m(z,r,t) = B_2(z,t)\frac{(n_c+n_f)}{n_m}\left(\frac{{r_2}^2}{r^2} - 1\right) r \tag{20.c}$$

$$\sigma_{rz_f}(z,r,t) = A_1(z,t)\, r \tag{21.a}$$

$$\sigma_{rz_c}(z,r,t) = A_1(z,t)\frac{n_f}{n_c}\left(\frac{{r_1}^2}{r^2} - 1\right) r - A_2(z,t)\frac{(1-n_m)}{n_c}\left(\frac{{r_0}^2}{r^2} - 1\right) r \tag{21.b}$$

$$\sigma_{rz_m}(z,r,t) = A_2(z,t)\frac{(n_c+n_f)}{n_m}\left(\frac{{r_2}^2}{r^2} - 1\right) r \tag{21.c}$$

Now, by identifying:

$$\zeta_1 = 2\, n_f\, A_1 \tag{22.a}$$

$$S_1 = 2\, n_f\, B_1 \tag{22.b}$$

$$\zeta_2 = 2\,(n_f + n_c)A_2 \tag{22.c}$$

$$S_2 = 2\,(n_f + n_c)B_2 \tag{22.d}$$

Also, apply the interface continuity and symmetry conditions of equation (11), equations (14)-(19) and (22) look like:

$$n_f \frac{\partial \overline{\sigma_{zf}}}{\partial z} = - 2\, n_f\, A_1 + n_f\, \rho_f\, \frac{\partial^2 \overline{u_f}}{\partial t^2} \tag{23}$$

$$n_c \frac{\partial \overline{\sigma_{zc}}}{\partial z} = - 2\, (n_f + n_c) A_2 + 2\, n_f\, A_1 + n_c\, \rho_c\, \frac{\partial^2 \overline{u_c}}{\partial t^2} \tag{24}$$

$$n_m \frac{\partial \overline{\sigma_{zm}}}{\partial z} = 2\, (n_f + n_c) A_2 + n_m\, \rho_m\, \frac{\partial^2 \overline{u_m}}{\partial t^2} \tag{25}$$

$$n_f \frac{\partial \overline{\sigma_{zf}}}{\partial z} = f_{12}\, 2\, n_f\, \frac{\partial B_1}{\partial z} + n_f\, f_{11} \frac{\partial^2 \overline{u_f}}{\partial z^2} \tag{26}$$

$$n_c \frac{\partial \overline{\sigma_{zc}}}{\partial z} = n_c c_{11} \frac{\partial \overline{u_c}}{\partial z^2} + c_{12}\left(2\, (n_f + n_c) \frac{\partial B_2}{\partial z} - 2\, n_f\, \frac{\partial B_1}{\partial z}\right) \tag{27}$$

$$n_m \frac{\partial \overline{\sigma_{zm}}}{\partial z} = - 2\, m_{12}\, (n_f + n_c) \frac{\partial B_2}{\partial z} + n_m\, m_{11} \frac{\partial^2 \overline{u_m}}{\partial z^2} \tag{28}$$

Finally, by equating the above equations to eliminate $\overline{\sigma_{zf}}$, $\overline{\sigma_{zc}}$ and $\overline{\sigma_{zm}}$. yields:

$$- 2\, n_f\, A_1 + n_f\, \rho_f\, \frac{\partial^2 \overline{u_f}}{\partial t^2} = f_{12}\, 2\, n_f\, \frac{\partial B_1}{\partial z} + n_f\, f_{11} \frac{\partial^2 \overline{u_f}}{\partial z^2} \tag{29}$$

$$- 2\, (n_f + n_c) A_2 + 2\, n_f\, A_1 + n_c\, \rho_c\, \frac{\partial^2 \overline{u_c}}{\partial t^2} = n_c c_{11} \frac{\partial^2 \overline{u_c}}{\partial z^2} + c_{12}\left(2\, (n_f + n_c) \frac{\partial B_2}{\partial z} - 2\, n_f\, \frac{\partial B_1}{\partial z}\right) \tag{30}$$

$$2\,(n_f + n_c)A_2 + n_m\,\rho_m\,\frac{\partial^2 \overline{u_m}}{\partial t^2} = -2\,m_{12}\,(n_f + n_c)\frac{\partial B_2}{\partial z} + n_m\,m_{11}\frac{\partial^2 \overline{u_m}}{\partial z^2}$$

(31)

Next, use the continuity relation of (11) and then integrate equation (10) by parts with equation (12) after multiplying the filling part by r^2, CNT by $(r^2 - r_1^2)$, and the matrix part by $(r^2 - r_2^2)$. Then, substitute the resulting equations in (20.a) for the filling to get the following equation:

$$\partial u = \left(\frac{A\,r}{f_{55}} - \frac{\partial B}{\partial z}\,r\right)\partial r \tag{32.a}$$

Now, multiply (23.a) by (r^2) and integrate as per (13.a) to get the filling strain relation as:

$$u_1{}^* - \overline{u_f} = \frac{r_0{}^2}{4}\left(\frac{A_1}{f_{55}} - \frac{\partial B_1}{\partial z}\right) \tag{32.b}$$

Then, we do the same for equation (20.b) and multiply by $(r^2 - r_1{}^2)$ and integrate as per (13.b) to get:

$(u_1{}^* - \overline{u_c})$ in term of B_1, B_2, A_1, and A_2. (See appendix (A)) (33)

Following the same procedure for the matrix and then by multiplying by $(r^2 - r_2{}^2)$ and integrate as per (13.c) to get:

$(u_2{}^* - \overline{u_m})$ in term of B_1, B_2, A_1, and A_2. (See appendix (B)) (34)

Also, from the continuity it is clear that:

$$u_2{}^* - u_1{}^* = \overline{u_c} \tag{35}$$

To get the final strain relations first eliminate $u_1{}^*$ from (23.b) and (24) to have $(\overline{u_c} - \overline{u_f})$ such that, (See appendix (C)), :

$$\overline{u_c} - \overline{u_f} = ž_0 \frac{\partial B_1}{\partial z} - \frac{\partial B_2}{\partial z} ž_1 - A_1\, ž_2 + A_2\, ž_3 + \frac{A_1}{f_{55}} ž_4 - \frac{\partial B_1}{\partial z} ž_4\ , \tag{36}$$

Then, from (34) and (35) to obtain:

$(u_2{}^* - \overline{u_m}\,)$ in term of B_1, B_2, m_{55}, A_1, and A_2. (See appendix (D)) (37)

Now, substitute the value of $u_1{}^*$ from (23) in (37) to get:

$(\,u_1{}^*)$ in term of $(\overline{u_c}\,)$, B_1, B_2, A_1, and A_2. (See appendix (E)) (38)

Finally, substitute (37) in (38) to get $(\,\overline{u_m} - 2\overline{u_c}\,)$ such that, (See appendix (F)),:

$$\overline{u_m} - 2\overline{u_c} = -\frac{\partial B_1}{\partial z} ž_5 + \frac{\partial B_2}{\partial z} (ž_6 + m_{55}\, ž_9) + A_1\, ž_7 - A_2\, (ž_8 + ž_9) \tag{39}$$

After analyzing the strains, the radial and tangential stresses should be analyzed as followed:

First, subtract the tangential stresses in the general form of equation (9) from equation (8) to get:

$$\sigma_r - \sigma_\theta = 2\, c_{55} \left(\frac{\partial v}{\partial r} - \frac{v}{r}\right) \qquad (40)$$

Second, the averaged σ_{rf}, σ_{rc} and σ_{rm} need to be eliminated from equation in order to gain and reach our final differential equations. In order to this, the constitutive equation number (8) needs to be specialized for the filling, CNTs and the matrix considering the equations (20) and (21).

Finally, eliminate the averaged stresses for the filling, CNTs and the matrix between achieved equations.

Now, let us solve it in details such that:

Specialize equation (40) and use the previous approximation to gain:

First for the filling:

$$\sigma_{rf} - \sigma_{\theta f} = 0 \qquad (41.a)$$

So,

$$\sigma_{rf} = \sigma_{\theta f} \qquad (41.b)$$

Then, for the CNT to get:

$$\sigma_{rc} - \sigma_{\theta c} = 4\, c_{55}\, \left(\frac{(B_1 - B_2)\, r_0{}^2}{(r_0{}^2 - r_1{}^2)\, r^2} \right) \tag{42}$$

Finally for the matrix, such that:

$$\sigma_{rm} - \sigma_{\theta m} = 4\, m_{55}\, \left(\frac{(B_2)\, r_1{}^2\;\, r_2{}^2}{(r_1{}^2 - r_2{}^2)\, r^2} \right) \tag{43}$$

Now, substitute (20) and (21) in (41), (42) and (43) and then in equation (2) for the filling, CNT, and matrix, respectively to get:

$$\sigma_{rf} - \sigma_{r\theta} = 2\, f_{55}(B_1 - \frac{v}{r}) \tag{44.a}$$

Then, substitute (35.a) in (2) to have:

$$\frac{\partial \sigma_{rf}}{\partial r} + \frac{\partial \sigma_{rz}}{\partial z} + \frac{1}{r}\,(2\, f_{55}(B_1 - \frac{v}{r})\,) = \rho_f\, \frac{\partial^2 v}{\partial t^2} \tag{44.b}$$

Now rearrange and multiply by (r^2) and average the result to get:

$$\sigma_{r1}{}^{*} - \overline{\sigma_{rf}} = \frac{r_0{}^2}{4}\, \left(\frac{\partial^2 B_1}{\partial t^2}\, \rho_c - \frac{\partial A_1}{\partial z}\right) \tag{44.c}$$

Then, rearrange and multiply by $(r^2 - r_1{}^2)$ and average to get:

$$(\sigma_{r1}{}^{*} - \overline{\sigma_{r_c}}) \text{ in term of } B_1, B_2, A_1, \text{ and } A_2. \text{ (See Appendix (G))} \tag{45}$$

Finally, follow the same procedure for the matrix by substituting (43) in (2) and then multiply by $(r^2 - r_2{}^2)$ to finally get:

$$(\sigma_{r2}{}^{*} - \overline{\sigma_{r_m}}) \text{ in term of } B_1, B_2, A_1, \text{ and } A_2. \text{ (See Appendix (H))} \tag{46}$$

Note also that:

$$\sigma_{r2}{}^{*} - \sigma_{r1}{}^{*} = \overline{\sigma_{r_c}} \tag{47}$$

Now, from (44.c) and (45):

$$(\overline{\sigma_{r_c}} - \overline{\sigma_{r_f}}) \text{ in term of } B_1, B_2, A_1, \text{ and } A_2. \text{ (See Appendix (I))} \tag{48}$$

Moreover, from (45), (46) and (47), we will get:

$$(\overline{\sigma_{r_m}} - 2\overline{\sigma_{r_c}}) \text{ in term of } B_1, B_2, A_1, \text{ and } A_2. \text{ (See Appendix (J))} \tag{49}$$

After that, $\overline{\sigma_{r_f}}, \overline{\sigma_{r_c}},$ and $\overline{\sigma_{r_m}}$ are needed to be eliminated in order to get the final pair of relations. This will be done firstly by specializing the constrictive equation no. (8) for the filling, CNT, and matrix and using (20) and (21) to end with the following:

$$\sigma_{r_f} = f_{12} \frac{\partial u}{\partial z} + B_1 \left(f_{12} + f_{12}\right) \tag{50}$$

$$\sigma_{r_c} = \{r^2 \ [c_{12} \ (r_0{}^2 - r_1{}^2) \frac{\partial u}{\partial z} + (B_1 r_0{}^2 - B_2 r_1{}^2) \ (c_{12} + c_{12})] - [(B_1 - B_2) \ (c_{12} - c_{12}) \ r_0{}^2 \ r_1{}^2 \ ] \} / [(r_0{}^2 - r_1{}^2) \ r^2] \tag{51}$$

$$\sigma_{r_m} = \{r^2 \ [m_{12} \ (r_1{}^2 - r_2{}^2) \frac{\partial u}{\partial z} + (B_2 r_1{}^2) \ (m_{12} + m_{12})] - [(B_2) \ (m_{12} - m_{12}) \ r_1{}^2 \ r_2{}^2 \ ] \} / [(r_1{}^2 - r_2{}^2) \ r^2] \tag{52}$$

After that, (50), (51), and (52) shall be averaged to get:

$$\overline{\sigma_{r_f}} = f_{12} \frac{\partial \overline{u_f}}{\partial z} + B_1 \left(f_{12} + f_{12}\right) \tag{53}$$

$$\overline{\sigma_{r_c}} = -\frac{1}{\frac{(r_1{}^2 - r_0{}^2)}{2}} \{ \ c_{12} \ (r_0{}^2 - r_1{}^2)^2 \ \frac{\partial \overline{u_c}}{\partial z} + c_{22} [\ B_1 \ r_0{}^2 (2 \ln(r_0) \ r_1{}^2 + r_0{}^2 - r_1{}^2 \ (\ 2 \ln(r_1) + 1) \ ) - B_2 \ (2 \ r_0{}^2 \ln(r_0) - r_0{}^2 \ (\ 2 \ln(r_1) - 1) - r_1{}^2) \ r_1{}^2] - c_{12} [\ B_1 \ r_0{}^2 (2 \ln(r_0) \ r_1{}^2 - r_0{}^2 - r_1{}^2 \ (\ 2 \ln(r_1) - 1) \ ) - B_2 \ (2 \ r_0{}^2 \ln(r_0) - r_0{}^2 \ (\ 2 \ln(r_1) + 1) + r_1{}^2) \ r_1{}^2] \} / [2 \ (r_0{}^2 - r_1{}^2) \tag{54}$$

$$\overline{\sigma_{r_m}} = -\frac{1}{\frac{(r_2{}^2 - r_1{}^2)}{2}} \{ \ m_{12} \ (r_1{}^2 - r_2{}^2)^2 \ \frac{\partial \overline{u_m}}{\partial z} + [\ m_{22} (2 \ln(r_1) \ r_2{}^2 + r_1{}^2 - r_2{}^2 \ (\ 2 \ln(r_2) + 1) \ ) - m_{12} \ (\ 2 \ln(r_1) \ r_2{}^2 - r_1{}^2 - r_2{}^2 \ (\ 2 \ln(r_2) - 1) \ ) \ ] \ B_2 \ r_1{}^2 \} \ / \ [2 \ (r_1{}^2 - r_2{}^2) \ ] \tag{55}$$

By rearranging the above equations (53) and (54), we will get the following:

$(\overline{\sigma_{r_c}} - \overline{\sigma_{r_f}})$ in term of B_1, B_2, A_1, and A_2.(See appendix K)) (56)

Also, from equations (54) and (55) to get:

$(\overline{\sigma_{r_c}} - \overline{\sigma_{r_f}})$ in term of B_1, B_2, A_1, and A_2.(See appendix L)) (57)

Finally, to get the last two equations, eliminate the stresses variables $\overline{\sigma_{r_f}}$, $\overline{\sigma_{r_c}}$, and $\overline{\sigma_{r_m}}$ from (47), (49), (56) and (57) to gain the required relation such that, (See appendix M),:

$$\frac{\partial^2 B_1}{\partial t^2}\rho_c - \frac{r_0{}^2}{4}\frac{\partial A_1}{\partial z} + \Omega_1\frac{\partial A_1}{\partial z} - \Omega_2\frac{\partial A_2}{\partial z} - \Omega_3\frac{\partial^2 B_1}{\partial t^2} + \Omega_4\frac{\partial^2 B_2}{\partial t^2} + \Omega_5 B_1 - \Omega_5 B_2 =$$

$$-\Omega_0\frac{\partial \overline{u_c}}{\partial z} - \Omega_6 B_1 + B_2\Omega_7 + \Omega_8 B_1 - \Omega_9 B_2 - f_{12}\frac{\partial \overline{u_f}}{\partial z} - B_1(f_{12} + f_{12}) \tag{58}$$

Also,

$$-¥_0\frac{\partial A_1}{\partial z} + ¥_1\frac{\partial A_2}{\partial z} + \frac{\partial^2 B_1}{\partial t^2}¥_2 - \frac{\partial^2 B_2}{\partial t^2}¥_3 - B_1 ¥_4 + B_2 ¥_4 + ¥_5\frac{\partial A_2}{\partial z} - \frac{\partial^2 B_2}{\partial t^2}¥_6 + B_2 ¥_7 =$$

$$-¥_8\frac{\partial \overline{u_m}}{\partial z} - ¥_9 B_2 + ¥_{10}\frac{\partial \overline{u_c}}{\partial z} + ¥_{11} B_1 - ¥_{12} B_2 - ¥_{13} B_1 + ¥_{14} B_2 \tag{59}$$

Lastly, from equations (29), (30), (31), (36), (39), (58) and (59), the composite system behavior is completely described. Those equations consist of four main partial differential equations which couple the longitudinal averaged displacements, the interfacial shear stress, and the interfacial radial displacement.

Steady state harmonic solution is going to be used in order to derive the characteristic dispersion of the NCT fiber matrix composite and find out its harmonic wave solution such that:

$$(\overline{u_f}, \overline{u_c}, \overline{u_m}, A_1, A_2, B_1, B_2) = (X_1, X_2, X_3, X_4, X_5, X_6, X_7)\ e^{i(kz-wt)} \qquad (60)$$

$$\begin{array}{c}
\begin{array}{ccccccc} \overline{u_f} & \overline{u_c} & \overline{u_m} & A_1 & A_2 & B_1 & B_2 \end{array} \\
\left[\begin{matrix}
n_f\,\rho_f\,w^2 - n_f\,f_{11}\,k^2 & 0 & 0 & 2\,n_f & 0 & 2\,f_{12}\,n_f & 0 \\
0 & n_c\,\rho_c\,w^2 - n_c\,c_{11}\,k^2 & 0 & -2\,n_f & 2\,(n_f + n_c) & -4\,c_{12}\,(n_f + n_c)\,n_f\,k & 2\,c_{12}(n_f + n_c)\,k \\
0 & 0 & n_m\,\rho_m w^2 - n_m\,m_{11} k^2 & 0 & -2\,(n_f + n_c) & 0 & -2\,m_{12}\,(n_f + n_c)\,k \\
1 & -1 & 0 & \frac{\check{z}_4}{f_{55}} - \check{z}_2 & \check{z}_3 & (\check{z}_0 - \check{z}_4)\,k & -\check{z}_1 k \\
0 & 2 & -1 & \check{z}_7 & -(\check{z}_8 + \check{z}_9) & -\check{z}_5 k & (\check{z}_6 + m_{55}\,\check{z}_9)k \\
-f_{12} k & -\Omega_0\,k & 0 & (\frac{r_0{}^2}{4} - \Omega_1)\,k & \Omega_2\,k & \Omega_8 - \Omega_6 - \Omega_5 - (f_{12} + f_{12}) - \left(-\rho_c \frac{r_0{}^2}{4} + \Omega_3\right) w^2 & \Omega_7 - \Omega_9 + \Omega_5 + \Omega_4\,w^2 \\
0 & \yen_{10}\,k & -\yen_8 k & \yen_0\,k & -(\yen_1 + \yen_5)\,k & \yen_4 + \yen_{11} - \yen_{13} + \yen_2 w^2 & \yen_{14} - \yen_9 - \yen_{12} - \yen_7 - \yen_4 - (\yen_6 + \yen_3)w^2
\end{matrix}\right]
\end{array}$$

Where **X** is the amplitude, **k** is the wave number, and **ω** is the circular frequency

CHAPTER VI

THE DEVELOPED CONTINUUM MIXTURE MODEL RESULTS

This section discusses the last results for the wave propagation of the embedded CNT fibrous composite. This chapter analyses the final matrix results of the averaged continuum model that describes the composite behaviors for both the nano and macro levels.

VI.I CNT Composites Results

First of all, the equations that describe the relation of radial and shear stress versus the embedded CNT fibrous composite radius is needed to be confirmed in order to make sure that they meet and comply with the continuity and constitutive assumption as stated in equation (11). These equations concern the radial dependence of the radial displacement and the shear stress. They are chosen to automatically satisfy the symmetry conditions which retain the integrity of the propagation in the individual filling, CNT, and matrix components subject to the interaction terms ζ and S.

So, the following assumed equations should be drawn:

$$v_f(z, r, t) = B_1(z, t)\, r$$

$$v_c(z,r,t) = B_1(z,t)\frac{n_f}{n_c}\left(\frac{r_1{}^2}{r^2}-1\right)r - B_2(z,t)\frac{(1-n_m)}{n_c}\left(\frac{r_0{}^2}{r^2}-1\right)r$$

$$v_m(z,r,t) = B_2(z,t)\frac{(n_c+n_f)}{n_m}\left(\frac{r_2{}^2}{r^2}-1\right)r$$

$$\sigma_{rz_f}(z,r,t) = A_1(z,t)\, r$$

$$\sigma_{rz_c}(z,r,t) = A_1(z,t)\frac{n_f}{n_c}\left(\frac{r_1{}^2}{r^2}-1\right)r - A_2(z,t)\frac{(1-n_m)}{n_c}\left(\frac{r_0{}^2}{r^2}-1\right)r$$

$$\sigma_{rz_m}(z,r,t) = A_2(z,t)\frac{(n_c+n_f)}{n_m}\left(\frac{r_2{}^2}{r^2}-1\right)r$$

Where,

$$\zeta_1 = 2\, n_f\, A_1 = \frac{2\, n_f \sigma_{rz1}{}^*}{r_0}$$

$$\zeta_2 = 2\,(n_f + n_c)A_2 = \frac{2\,(n_f + n_c)\sigma_{rz2}{}^*}{r_1}$$

$$S_1 = 2\, n_f\, B_1 = \frac{2\, n_f v_1{}^*}{r_0}$$

$$S_2 = \frac{2\,(n_f + n_c)v_2{}^*}{r_1} = 2\,(n_f + n_c)B_2$$

This thesis will examine the continuity equations by plotting and comparing the radial stress continuity relations for a composite which is having an air as a filling.

In this thesis, the composite dimensional properties are going to be estimated as:

r_0= 2 nm, r_1= 2.34 nm, r_2 = 8.34 nm. Hence, the shape of the above radial stress continuity relations are plot using the MatLab program as shown in appendix (N) and appendix (O).

Consequently, the general shape as in the filling, the carbon nanotube and the matrix, respectively, are shown in the following figures:

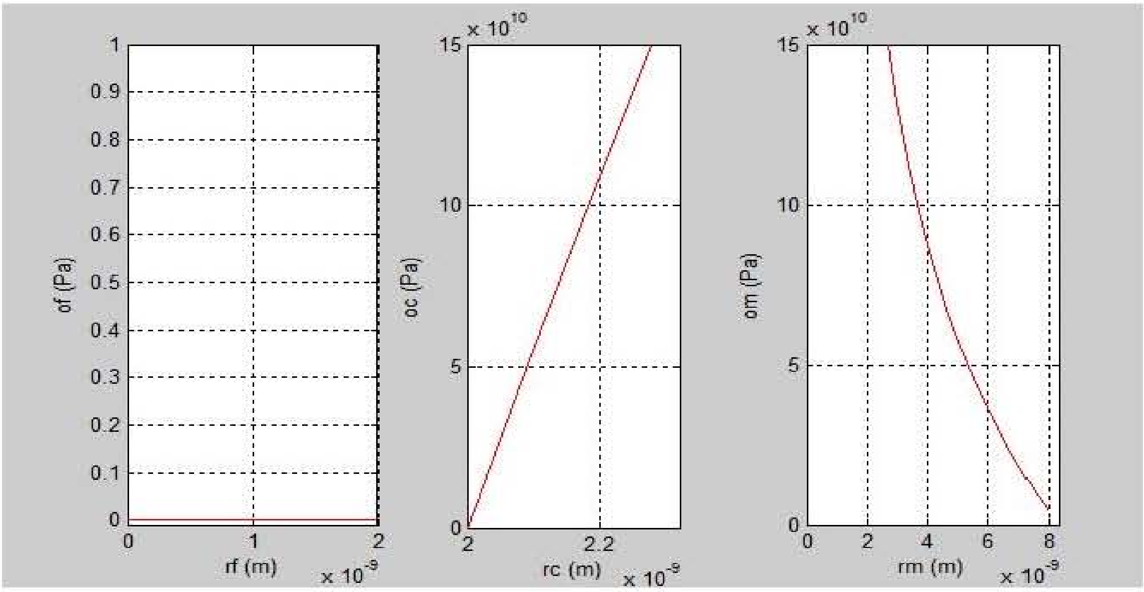

Figure 7: Continuity of (σ) along (r) for the embedded CNT composite in the case that composite is filled with air.

The above figures represent the continuity and constitutive assumption exactly as stated in equation (11). They are showing the continuity along the composite. Because the composite is filled with air, it is clear that σ_{rz_f} is equal to zero along the composite. Note also that because the CNT has very small radius along the composite, its shape is almost linear. Finally, σ_{rz_c} returns to zero such that it verifies the continuity.

Second, the general wave model for the embedded CNT composite that is described by equation (60) must be solved. To solve this matrix with nontrivial solution, the determinant must be zero. Therefore, we are going to use the MATLAB program to reach our final solutions. Hence, by having the required phase velocity of each mode is defined as C= ω/k, then, the dispersion curves of each mode of the CNT composite can be finally drawn.

In this study, the filling is assumed to be air. Also, the following CNT, and matrix properties are used in order to get the dispersion curves and the mixture modes:

r_0 = 1 nm

r_1 = 1.34 nm

r_2 = 5.34 nm

Carbon nanotube Young's modulus = 1.12 Tpa

Poisson ratio for the carbon nanotube = 0.3

Therefore,

$$c_{11} = \frac{E}{(1-v^2)}, \qquad c_{12} = \frac{E*v}{(1-v^2)}, \qquad c_{44} = \frac{E*v}{2*(1+v^2)}$$

And for the matrix, the following properties are going to be assumed [55]:

$$m_{ij} = \begin{bmatrix} 193.3 & 103.0 & 103.0 & 0 & 0 & 0 \\ 103.0 & 193.3 & 103.0 & 0 & 0 & 0 \\ 103.0 & 103.0 & 193.3 & 0 & 0 & 0 \\ 0 & 0 & 0 & 45 & 0 & 0 \\ 0 & 0 & 0 & 0 & 45 & 0 \\ 0 & 0 & 0 & 0 & 0 & 45 \end{bmatrix} . \quad \text{Gpa}$$

So, by using the MatLab program, in this special case we will have six different solutions of $(\boldsymbol{w})$ as functions of $(\boldsymbol{k})$, (see appendix (C)). These resulting equations represent six solutions for $(\boldsymbol{k})$ for a given frequency. Hence, solutions for k occur in three pairs, and each pair having two k's that is actually negative of each other. Consequently, three values of k represent three wave numbers for three modes propagating in the positive (z) direction, while the others represent three wave numbers of three modes that are propagating in the negative (z) direction.

Therefore, each of the three moods is drawn as follows:

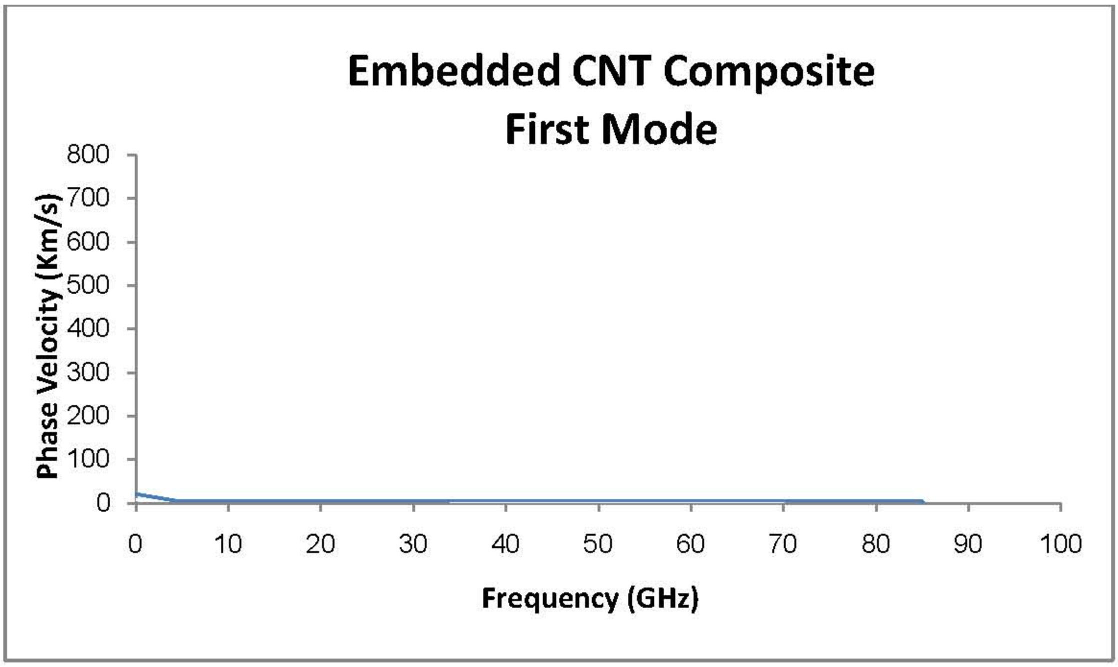

Figure 8: first mode of the embedded CNT composite mixture models.

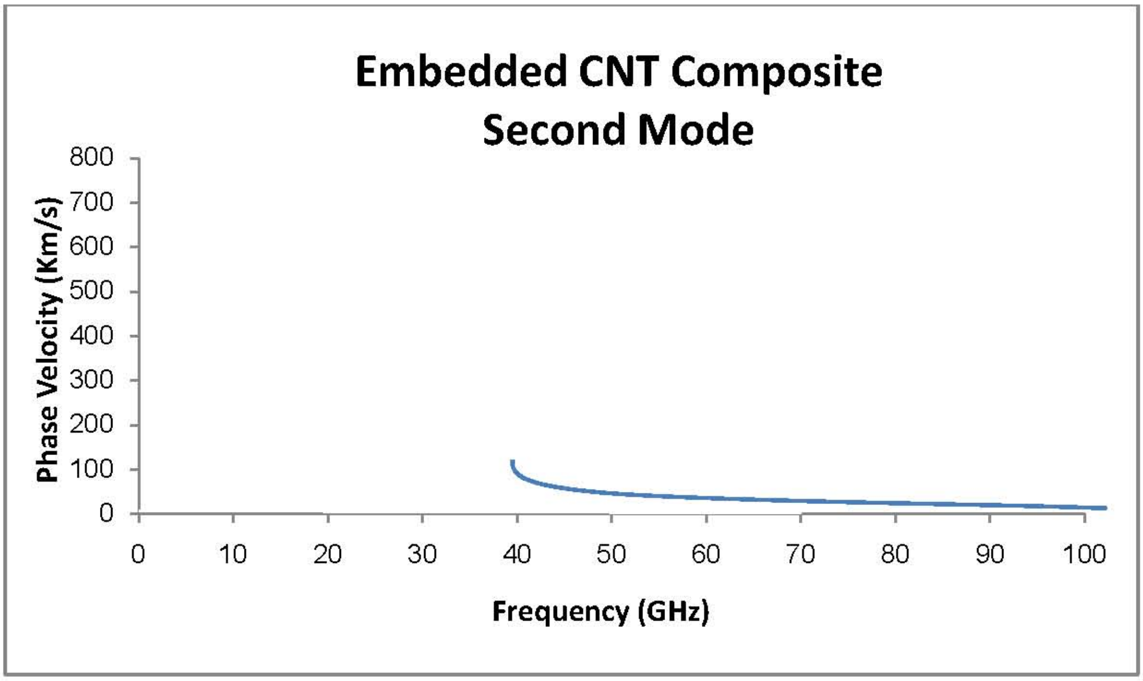

Figure 9: second mode of the embedded CNT composite mixture models.

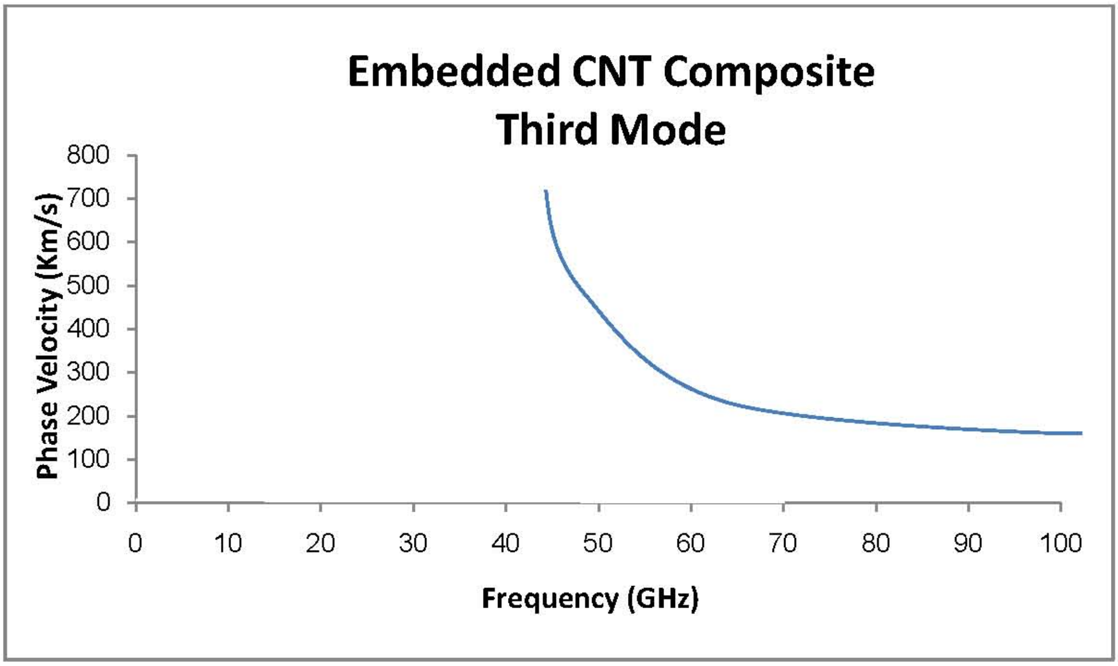

Figure 10: third mode of the embedded CNT composite mixture models.

Clearly, the last three figures represent the final solution of the modes of the embedded CNT composites by using the continuum mixture models. The frequency-dependent dispersion curves shown in figure (8), figure (9), and (10) are essentially valid for low frequency ranges, as these figures demonstrate. The highest value of the phase velocity (C) for each mode represents our composite behavior as if it is made totally form the CNTs. On the other hand, each mode converges at the value that represents our composite behavior as if it is made totally form the matrix without embedding CNTs. Also, the high-frequency limits indicate effective bulk waves having wave speeds that are either pure or combinations depending on the types of the properties of the CNT and matrix.

VI.II Macro Composites Results

In order to guarantee the validity of our results, the macro level composites should be also considered and their properties should be verified. The following fiber and matrix properties from reference [55] are going to be used in order to get the dispersion curves and the mixture modes:

$$f_{ij} = \begin{bmatrix} 381.3 & 58.24 & 58.24 & 0 & 0 & 0 \\ 58.24 & 262.8 & 65.20 & 0 & 0 & 0 \\ 58.24 & 65.20 & 262.8 & 0 & 0 & 0 \\ 0 & 0 & 0 & 37.29 & 0 & 0 \\ 0 & 0 & 0 & 0 & 65.35 & 0 \\ 0 & 0 & 0 & 0 & 0 & 65.35 \end{bmatrix} \quad \text{Gpa}$$

$$m_{ij} = \begin{bmatrix} 193.3 & 103.0 & 103.0 & 0 & 0 & 0 \\ 103.0 & 193.3 & 103.0 & 0 & 0 & 0 \\ 103.0 & 103.0 & 193.3 & 0 & 0 & 0 \\ 0 & 0 & 0 & 45 & 0 & 0 \\ 0 & 0 & 0 & 0 & 45 & 0 \\ 0 & 0 & 0 & 0 & 0 & 45 \end{bmatrix} \text{Gpa}$$

Where;

Matrix radius = r_2 = 132.3 µm, fiber radius = r_1 = 66 µm, and r_0 = 0 for this case. Therefore, MatLab program is used here as illustrated in appendix (P). Consequently, the final modes results are achieved as:

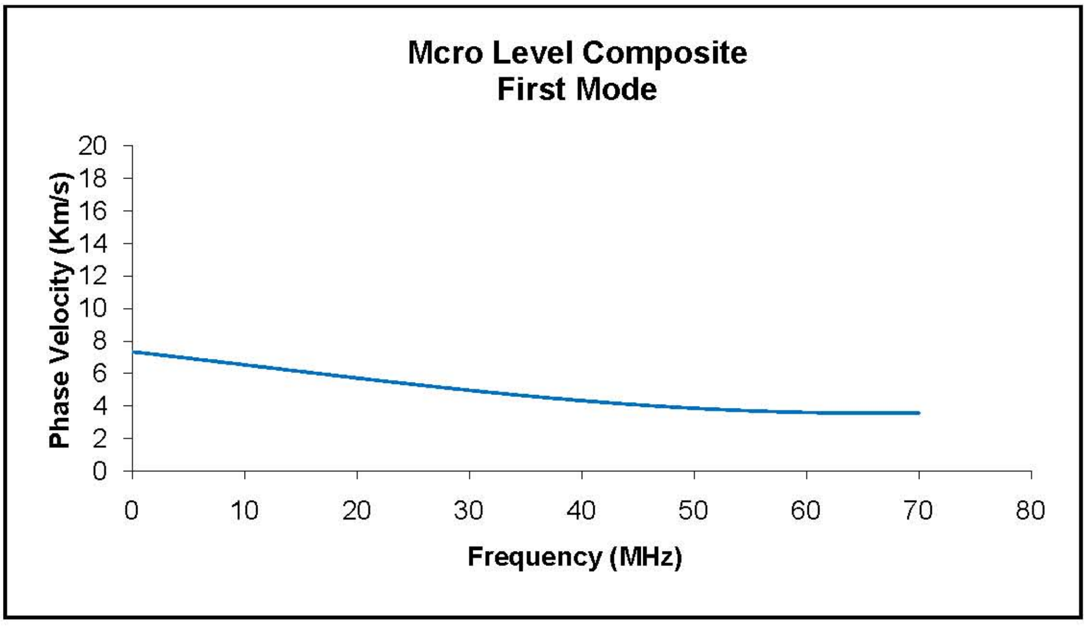

Figure 11: fundamental mode of the macro composite using improved mixture models.

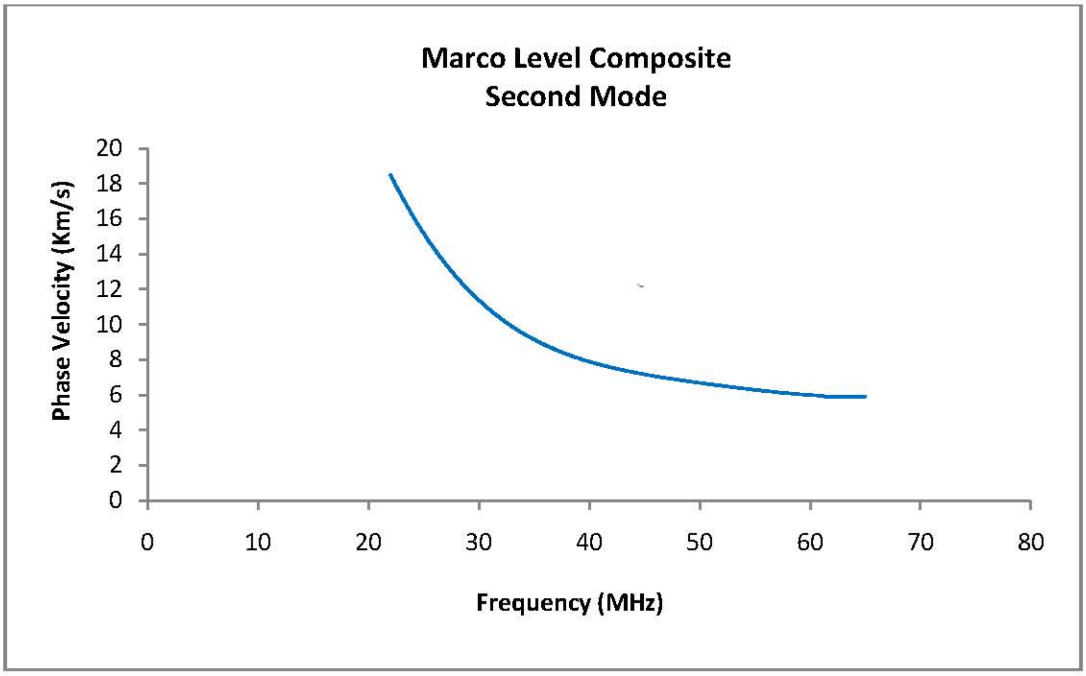

Figure 12: The second mode of the macro composite using improved mixture models.

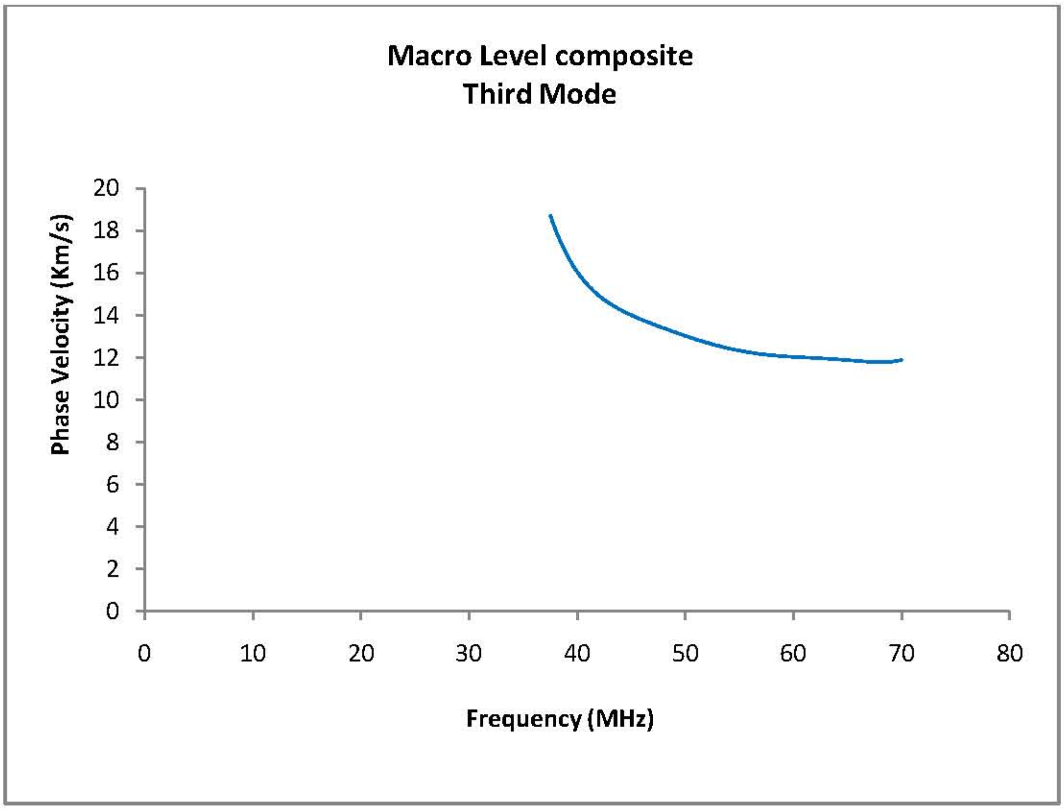

Figure 13: The third mode of the macro composite using improved mixture models.

The frequency-dependent dispersion curves shown in figures (11), (12) and (13) are essentially valid for low frequency ranges, as these figures demonstrate. The high-frequency limits indicate effective bulk waves having wave speeds that are either pure or combinations depending on the types of the properties of the fiber and matrix. The improved averaged model method predicts three bulk wave limits; that are, two for pure longitudinal and one for a mixture shear.

Finally, the improved mixture continuum model is needed to be tested by using the experimental data of the same composite as illustrated in Reference [55]:

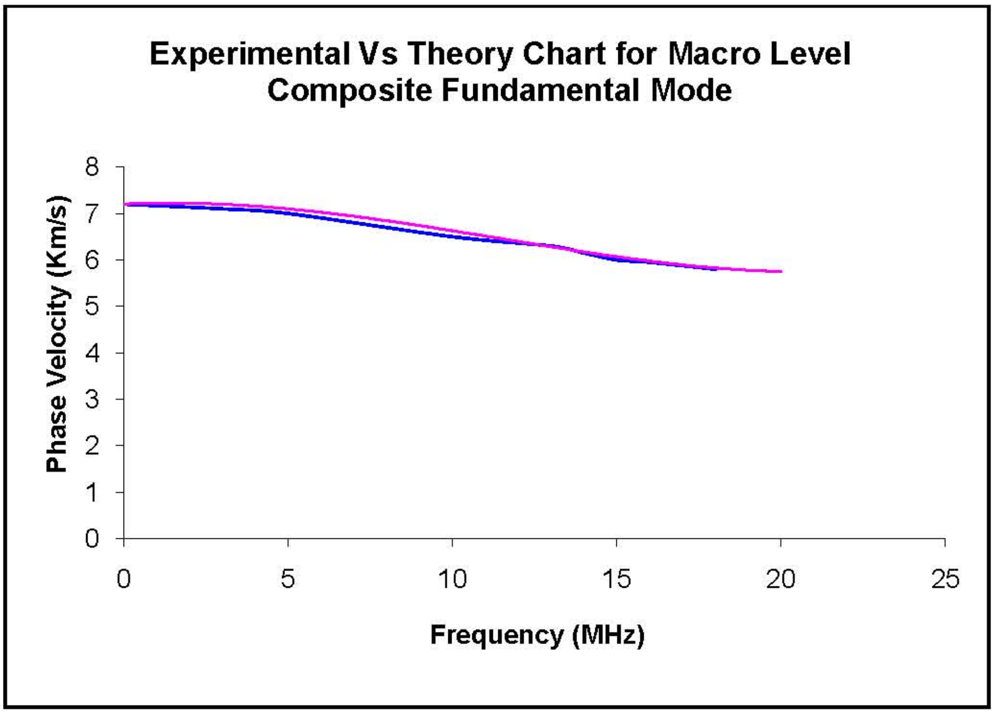

Figure 14: The fundamental mode comparisons of the macro composite using improved mixture models and the experimental data.

So, in Figure (14), the frequency dependence of the fundamental mode is plotted and compared with results obtained from the experimental data. It is clear that, significant and accurate results are achieved by the improved mixture model when compared with the experimental data.

In each graph, the highest value of the phase velocity (C) for each mode represents composite behavior as if it is made totally form the fibrous materials. On the other hand, each mode converges at the value that represents our composite behavior if it is made totally form the matrix without embedding the fibers. Also, the high-frequency limits indicate effective bulk waves having wave speeds that are either pure or combinations depending on the types of the properties of the fiber and matrix.

As a result, our averaged continuum model is valid for both nano and micro composite levels. Moreover, it can give very accurate results for composite behaviors. Besides, it is clear from the comparison between our CNT composite figures (8)-(10), and our macro composite figures (11)-(13), that the phase velocity for the CNT composite are much more higher and has higher frequencies ranges as expected.

Since CNT composite has higher phase velocity, it has higher energy and hence it has higher strength than the macro level composite. Note also that the CNT matrix has the same properties of the macro level composites matrix. However, the phase velocity of the CNT composite converges to higher value than the convergence of the macro composite. Therefore, it can be concluded from the graphs that as the matrix radius increases, its phase velocity decreases and hence its strength also decreases. On the other hand, it can be also concluded that as the radius of the embedded material, which has more strength than the matrix, increases, the composite strength also increases.

CHAPTER VII

CONCLUSION

In this work, the nanotechnology was define in general, and followed by the detailed description, properties, classifications, and applications of the CNTs. Subsequently, the two general modeling methods for analyzing the CNTs properties and responds were elucidated. These modeling methods are "atomic modeling" and the second modeling technique is the "continuum modeling". After that, the theory of "continuum mechanics" in general was introduced. Moreover, the model advantages, approaches, and principle were explained.

Then, this thesis explained in detailed the full procedure of getting the wave model for the CNTs using the Averaging Method for embedded CNT mixture composites. This procedure included the subsequent steps:

1. Finding the two cylindrical coordinate momentum equations in addition to the constitutive relations for each component in the composite.
2. Assessing the symmetry conditions, and evaluating the continuity of the stresses, shears, and deformations around the composite radius.
3. Averaging the momentum equations.
4. Deriving the relevant partial differential equations that describe the system in terms of the interactions term (ζ and S) and axial displacements (u), which also acquires finding the radial dependence of the shear stress and the radial displacement.

5. Applying the interface continuity and symmetry conditions for the stresses again along the composites in order to eliminate the stress and get the strains relations along the composites.
6. Analyzing the radial and tangential stresses, averaging them, and finally equating the tangential stresses and eliminating the radial stress.
7. Getting the final equation form steps (5) and (6) that describe the composite behavior.
8. Using the steady state harmonic in order to derive the characteristic dispersion of composite and find its harmonic wave solution.
9. Drawing the dispersion curves as a function of their frequencies for all the composite modes.

Finally, the embedded CNT composite wave propagation behaviors were established. Moreover, the wave propagation behaviors were also found for the micro level composites. Both nano and micro results show that the frequency-dependent dispersion curves are essentially valid for low frequency ranges. Also, it is clear from the comparison between our CNT composite figures (8)-(10), and our macro composite figures (11)-(13), that the phase velocity for the CNT composite are much more higher and has higher frequencies ranges and hence has higher values of energy and strength. Moreover, the high-frequency limits indicate effective bulk waves having wave speeds that are either pure or combinations depending on the types of the properties of the filling, embedded materials and matrix. Therefore, the averaged continuum model can give very accurate results for composite behaviors.

APPENDIX

A. $(u_1{}^* - \overline{u_c})$ in term of B_1, B_2, c_{55}, A_1, and A_2

$u_1{}^* - \overline{u_c}$ = - $\{\frac{\partial B_1}{\partial z}$ c_{55} $r_0{}^2$ [4 ln(r_0) $r_1{}^4$ + $r_0{}^4$ - 4 $r_0{}^2$ $r_1{}^2$ - $r_1{}^4$ (4 ln(r_1)-3)] - $\frac{\partial B_2}{\partial z}$ c_{55} [4 $r_0{}^2$ ln(r_0) $r_1{}^2$ - $r_0{}^4$ - 4 $r_0{}^2$ $r_1{}^2$ ln(r_1) + $r_1{}^4$] $r_1{}^2$- $A_1 r_0{}^2$ [4 ln(r_0) $r_1{}^4$ + $r_0{}^4$ - 4 $r_0{}^2$ $r_1{}^2$ - $r_1{}^4$ (4 ln (r_1)-3)] + A_2 [4 $r_0{}^2$ ln(r_0) $r_1{}^2$ - $r_0{}^4$ - 4 $r_0{}^2$ $r_1{}^2$ ln(r_1) + $r_1{}^4$] $r_1{}^2$ } / [4 c_{55} $(r_0{}^2 - r_1{}^2)$ ^{2}]

B. $(u_2{}^* - \overline{u_m})$ in term of B_1, B_2, c_{55}, A_1, and A_2

$u_2{}^* - \overline{u_m}$ = $(A_2 - \frac{\partial B_2}{\partial z}$ $m_{55})$ $r_1{}^2$ [4 ln(r_1) $r_2{}^4$ + $r_1{}^4$ - 4 $r_1{}^2$ $r_2{}^2$ - $r_2{}^4$ (4 ln(r_2)-3)] / [4 m_{55} $(r_1{}^2 - r_2{}^2)$ ^{2}]

C. $(\overline{u_c} - \overline{u_f})$ in term of B_1, B_2, c_{55}, A_1, and A_2

$\overline{u_c} - \overline{u_f}$ = {[$\frac{\partial B_1}{\partial z}$ c_{55} $r_0{}^2$ [4 ln(r_0) $r_1{}^4$ + $r_0{}^4$ - 4 $r_0{}^2$ $r_1{}^2$ - $r_1{}^4$ (4 ln(r_1)-3)] - $\frac{\partial B_2}{\partial z}$ c_{55} [4 $r_0{}^2$ ln(r_0) $r_1{}^2$ - $r_0{}^4$ - 4 $r_0{}^2$ $r_1{}^2$ ln(r_1) + $r_1{}^4$] $r_1{}^2$- $A_1 r_0{}^2$ [4 ln(r_0) $r_1{}^4$ + $r_0{}^4$ - 4 $r_0{}^2$ $r_1{}^2$ - $r_1{}^4$ (4 ln(r_1)-3)] + A_2 [4 $r_0{}^2$ ln(r_0) $r_1{}^2$ - $r_0{}^4$ - 4 $r_0{}^2$ $r_1{}^2$ ln(r_1) + $r_1{}^4$] $r_1{}^2$] / [4 c_{55} $(r_0{}^2 - r_1{}^2)$ ^{2}] } + {$\frac{r_0{}^2}{4}$ $(\frac{A}{f_{55}} - \frac{\partial B_1}{\partial z})$ }

For simplicity, this equation needs to be simplified by identifying the following variables as:

$\check{z}_0$= [$c_{55}\, r_0^{\,2}$ [4 ln(r_0) $r_1^{\,4}$ + $r_0^{\,4}$ - 4 $r_0^{\,2}\, r_1^{\,2}$ - $r_1^{\,4}$ (4 ln(r_1)-3)] / [4 c_{55} $(r_0^{\,2} - r_1^{\,2}\,)^{\,2}$]

$\check{z}_1$= c_{55} [4 $r_0^{\,2}$ ln(r_0) $r_1^{\,2}$ - $r_0^{\,4}$ - 4 $r_0^{\,2}\, r_1^{\,2}$ ln(r_1) + $r_1^{\,4}$] $r_1^{\,2}$ / [4 c_{55} $(r_0^{\,2} - r_1^{\,2}\,)^{\,2}$] $\check{z}_2$= $r_0^{\,2}$ [4 ln(r_0) $r_1^{\,4}$ + $r_0^{\,4}$ - 4 $r_0^{\,2}\, r_1^{\,2}$ - $r_1^{\,4}$ (4 ln(r_1)-3)] / [4 c_{55} $(r_0^{\,2} - r_1^{\,2}\,)^{\,2}$]

$\check{z}_3$= A_2 [4 $r_0^{\,2}$ ln(r_0) $r_1^{\,2}$ - $r_0^{\,4}$ - 4 $r_0^{\,2}\, r_1^{\,2}$ ln(r_1) + $r_1^{\,4}$] $r_1^{\,2}$ / [4 c_{55} $(r_0^{\,2} - r_1^{\,2}\,)^{\,2}$]

$\check{z}_4 = \frac{r_0^{\,2}}{4}$

So the main equation here will be simplified as:

$$\overline{u_c} - \overline{u_f} = \check{z}_0 \frac{\partial B_1}{\partial z} - \frac{\partial B_2}{\partial z} \check{z}_1 - A_1\, \check{z}_2 + A_2\, \check{z}_3 + \frac{A_1}{f_{55}} \check{z}_4 - \frac{\partial B_1}{\partial z} \check{z}_4$$

D. $(u_2^{\,*} - \overline{u_m}\,)$ in term of B_1, B_2, m_{55}, A_1, and A_2

$u_2^{\,*} - \overline{u_m} = (\overline{u_c} + u_1^{\,*}) - \overline{u_m} = (A_2 - \frac{\partial B_2}{\partial z} m_{55})\ r_1^{\,2}$ [4 ln(r_1) $r_2^{\,4}$ + $r_1^{\,4}$ - 4 $r_1^{\,2}\, r_2^{\,2}$ - $r_2^{\,4}$ (4 ln(r_2)-3)] / [4 m_{55} $(r_1^{\,2} - r_2^{\,2}\,)^{\,2}$]

E. ($\boldsymbol{u_1}^*$) in term of ($\overline{\boldsymbol{u_c}}$), $\boldsymbol{B_1}$, $\boldsymbol{B_2} \boldsymbol{A_1}$, and $\boldsymbol{A_2}$

$u_1{}^* = \overline{u_c}$ – { $\frac{\partial B_1}{\partial z}$ c_{55} $r_0{}^2$ [4 ln(r_0) $r_1{}^4$ + $r_0{}^4$ - 4 $r_0{}^2$ $r_1{}^2$ - $r_1{}^4$ (4 ln(r_1)-3)] - $\frac{\partial B_2}{\partial z}$ c_{55} [4 $r_0{}^2$ ln(r_0) $r_1{}^2$ - $r_0{}^4$ - 4 $r_0{}^2$ $r_1{}^2$ ln(r_1) + $r_1{}^4$] $r_1{}^2$- $A_1 r_0{}^2$ [4 ln(r_0) $r_1{}^4$ + $r_0{}^4$ - 4 $r_0{}^2$ $r_1{}^2$ - $r_1{}^4$ (4 ln(r_1)-3)] + A_2 [4 $r_0{}^2$ ln(r_0) $r_1{}^2$ - $r_0{}^4$ - 4 $r_0{}^2$ $r_1{}^2$ ln(r_1) + $r_1{}^4$] $r_1{}^2$ } / [4 c_{55} $(r_0{}^2 - r_1{}^2)^2$]

F. ($\overline{\boldsymbol{u_m}}$ – $2\overline{\boldsymbol{u_c}}$) in term of $\boldsymbol{B_1}$, $\boldsymbol{B_2}$, $\boldsymbol{A_1}$, and $\boldsymbol{A_2}$

$\overline{u_m}$ – $2\overline{u_c}$= { - [$\frac{\partial B_1}{\partial z}$ c_{55} $r_0{}^2$ [4 ln(r_0) $r_1{}^4$ + $r_0{}^4$ - 4 $r_0{}^2$ $r_1{}^2$ - $r_1{}^4$ (4 ln(r_1)-3)] - $\frac{\partial B_2}{\partial z}$ c_{55} [4 $r_0{}^2$ ln(r_0) $r_1{}^2$ - $r_0{}^4$ - 4 $r_0{}^2$ $r_1{}^2$ ln(r_1) + $r_1{}^4$] $r_1{}^2$- $A_1 r_0{}^2$ [4 ln(r_0) $r_1{}^4$ + $r_0{}^4$ - 4 $r_0{}^2$ $r_1{}^2$ - $r_1{}^4$ (4 ln(r_1)-3)] + A_2 [4 $r_0{}^2$ ln(r_0) $r_1{}^2$ - $r_0{}^4$ - 4 $r_0{}^2$ $r_1{}^2$ ln(r_1) + $r_1{}^4$] $r_1{}^2$] / [4 c_{55} $(r_0{}^2 - r_1{}^2)^2$] } - {($A_2 - \frac{\partial B_2}{\partial z}$ m_{55}) $r_1{}^2$ [4 ln(r_1) $r_2{}^4$ + $r_1{}^4$ - 4 $r_1{}^2$ $r_2{}^2$ - $r_2{}^4$ (4 ln(r_2)-3)] / [4 m_{55} $(r_1{}^2 - r_2{}^2)^2$] }

For simplicity, this equation needs to be simplified by identifying the following variables such that:

ž5= [c_{55} $r_0{}^2$ [4 ln(r_0) $r_1{}^4$ + $r_0{}^4$ - 4 $r_0{}^2$ $r_1{}^2$ - $r_1{}^4$ (4 ln(r_1)-3)] / [4 c_{55} $(r_0{}^2 - r_1{}^2)^2$]

ž6= [c_{55} [4 $r_0{}^2$ ln(r_0) $r_1{}^2$ - $r_0{}^4$ - 4 $r_0{}^2$ $r_1{}^2$ ln(r_1) + $r_1{}^4$] $r_1{}^2$] / [4 c_{55} $(r_0{}^2 - r_1{}^2)^2$]

ž7= $r_0{}^2$ [4 ln(r_0) $r_1{}^4$ + $r_0{}^4$ - 4 $r_0{}^2$ $r_1{}^2$ - $r_1{}^4$ (4 ln(r_1)-3)] / [4 c_{55} $(r_0{}^2 - r_1{}^2)^2$]

ž8= [4 $r_0{}^2$ ln(r_0) $r_1{}^2$ - $r_0{}^4$ - 4 $r_0{}^2$ $r_1{}^2$ ln(r_1) + $r_1{}^4$] $r_1{}^2$ / [4 c_{55} $(r_0{}^2 - r_1{}^2)^2$]

ž9 = $r_1{}^2$ [4 ln(r_1) $r_2{}^4$ + $r_1{}^4$ - 4 $r_1{}^2$ $r_2{}^2$ - $r_2{}^4$ (4 ln(r_2)-3)] / [4 m_{55} $(r_1{}^2 - r_2{}^2)^2$]

So, the main equation will be simplified as:

$\overline{u_m} - 2\overline{u_c} = - \frac{\partial B_1}{\partial z}$ ž$_5$ + $\frac{\partial B_2}{\partial z}$ (ž$_6$ + m_{55} ž$_9$) + A_1 ž$_7$ - A_2 (ž$_8$ + ž$_9$)

G. ($\boldsymbol{\sigma_{r1}}^* - \overline{\boldsymbol{\sigma_{r_c}}}$) in term of $\boldsymbol{B_1}$, $\boldsymbol{B_2}$, $\boldsymbol{A_1}$, and $\boldsymbol{A_2}$

$\sigma_{r1}{}^* - \overline{\sigma_{r_c}} =$ - { $\frac{\partial A_1}{\partial z}$ $r_0{}^2$ [2 ln($r_0{}^2$) $r_1{}^4$ + $r_0{}^4$ - 4 $r_0{}^2$ $r_1{}^2$ - $r_1{}^4$ (2 ln($r_1{}^2$)-3)] -

$\frac{\partial A_2}{\partial z}$ [2 $r_0{}^2$ ln($r_0{}^2$) $r_1{}^2$ - $r_0{}^4$ - 2 $r_0{}^2$ $r_1{}^2$ ln($r_1{}^2$) + $r_1{}^4$] $r_1{}^2$- $\frac{\partial^2 B_1}{\partial t^2}$ ρ_c $r_0{}^2$ [2 ln($r_0{}^2$) $r_1{}^4$ +

$r_0{}^4$ - 4 $r_0{}^2$ $r_1{}^2$ - $r_1{}^4$ (2 ln($r_1{}^2$)-3)] + $\frac{\partial^2 B_2}{\partial t^2}$ ρ_c [2 $r_0{}^2$ ln($r_0{}^2$) $r_1{}^2$ - $r_0{}^4$ - 4 $r_0{}^2$ $r_1{}^2$ ln($r_1{}^2$)

+ $r_1{}^4$] $r_1{}^2$ + 8 ($B_1 - B_2$) c_{55} [$r_0{}^2$ ln($r_0{}^2$) $-$ $r_0{}^2$[ln($r_1{}^2$) + 1] + $r_1{}^2$] } / [4 ($r_0{}^2 - r_1{}^2$) ^{2}

]

H. ($\boldsymbol{\sigma_{r2}}^* - \overline{\boldsymbol{\sigma_{r_m}}}$) in term of $\boldsymbol{B_1}$, $\boldsymbol{B_2}$, $\boldsymbol{A_1}$, and $\boldsymbol{A_2}$

$\sigma_{r2}{}^* - \overline{\sigma_{r_m}} =$ - { $\frac{\partial A_2}{\partial z}$ $r_1{}^2$ [2 ln($r_1{}^2$) $r_2{}^4$ + $r_1{}^4$ - 4 $r_1{}^2$ $r_2{}^2$ - $r_2{}^4$ (2 ln($r_2{}^2$)-3)] - $\frac{\partial^2 B_2}{\partial t^2}$ $r_1{}^2$

ρ_m [2 ln($r_1{}^2$) $r_2{}^4$ -$r_1{}^4$ - 4 $r_1{}^2$ $r_2{}^2$ $-$ $r_2{}^4$ [2 ln($r_2{}^2$) -3]]+ 8 (B_2) m_{55} [$r_1{}^2$ ln($r_1{}^2$) $-$

$r_1{}^2$[ln($r_2{}^2$) + 1] + $r_2{}^2$] $r_2{}^2$ } / [4 ($r_1{}^2 - r_2{}^2$) ^{2}]

I. $(\overline{\sigma_{r_c}} - \overline{\sigma_{r_f}})$ in term of B_1, B_2, A_1, and A_2

$\overline{\sigma_{r_c}} - \overline{\sigma_{r_f}} = \frac{r_0^2}{4} (\frac{\partial^2 B_1}{\partial t^2} \rho_c - \frac{\partial A_1}{\partial z}) + \{ \frac{\partial A_1}{\partial z} r_0^2 [2 \ln(r_0^2) r_1^4 + r_0^4 - 4 r_0^2 r_1^2 - r_1^4 (2 \ln(r_1^2)-3)] - \frac{\partial A_2}{\partial z} [2 r_0^2 \ln(r_0^2) r_1^2 - r_0^4 - 2 r_0^2 r_1^2 \ln(r_1^2) + r_1^4] r_1^2 - \frac{\partial^2 B_1}{\partial t^2} \rho_c r_0^2 [2 \ln(r_0^2) r_1^4 + r_0^4 - 4 r_0^2 r_1^2 - r_1^4 (2 \ln(r_1^2)-3)] + \frac{\partial^2 B_2}{\partial t^2} \rho_c [2 r_0^2 \ln(r_0^2) r_1^2 - r_0^4 - 4 r_0^2 r_1^2 \ln(r_1^2) + r_1^4] r_1^2 + 8 (B_1 - B_2) c_{55} [r_0^2 \ln(r_0^2) - r_0^2 [\ln(r_1^2) + 1] + r_1^2] \} / [4 (r_0^2 - r_1^2)^2]$

J. $(\overline{\sigma_{r_m}} - 2\overline{\sigma_{r_c}})$ in term of B_1, B_2, A_1, and A_2

$\overline{\sigma_{r_m}} - 2\overline{\sigma_{r_c}} = - \{ \frac{\partial A_1}{\partial z} r_0^2 [2 \ln(r_0^2) r_1^4 + r_0^4 - 4 r_0^2 r_1^2 - r_1^4 (2 \ln(r_1^2)-3)] - \frac{\partial A_2}{\partial z} [2 r_0^2 \ln(r_0^2) r_1^2 - r_0^4 - 2 r_0^2 r_1^2 \ln(r_1^2) + r_1^4] r_1^2 - \frac{\partial^2 B_1}{\partial t^2} \rho_c r_0^2 [2 \ln(r_0^2) r_1^4 + r_0^4 - 4 r_0^2 r_1^2 - r_1^4 (2 \ln(r_1^2)-3)] + \frac{\partial^2 B_2}{\partial t^2} \rho_c [2 r_0^2 \ln(r_0^2) r_1^2 - r_0^4 - 4 r_0^2 r_1^2 \ln(r_1^2) + r_1^4] r_1^2 + 8 (B_1 - B_2) c_{55} [r_0^2 \ln(r_0^2) - r_0^2 [\ln(r_1^2) + 1] + r_1^2]] / [4 (r_0^2 - r_1^2)^2] + [\frac{\partial A_2}{\partial z} r_1^2 [2 \ln(r_1^2) r_2^4 + r_1^4 - 4 r_1^2 r_2^2 - r_2^4 (2 \ln(r_2^2)-3)] - \frac{\partial^2 B_2}{\partial t^2} r_1^2 \rho_m [2 \ln(r_1^2) r_2^4 - r_1^4 - 4 r_1^2 r_2^2 - r_2^4 [2 \ln(r_2^2) -3]] + 8 (B_2) m_{55} [r_1^2 \ln(r_1^2) - r_1^2 [\ln(r_2^2) + 1] + r_2^2] r_2^2 \} / [4 (r_1^2 - r_2^2)^2]$

K. $(\overline{\sigma_{r_c}} - \overline{\sigma_{r_f}})$ **in term of** B_1, B_2, A_1, **and** A_2

$\overline{\sigma_{r}}_{c} - \overline{\sigma_{r}}_{f} = -\frac{1}{\frac{(r_1{}^2-r_0{}^2)}{2}}\{\, c_{12}\ (r_0{}^2 - r_1{}^2)^2\ \frac{\partial \overline{u_c}}{\partial z} + c_{22}[\, B_1\, r_0{}^2(2\ln(r_0)\, r_1{}^2 + r_0{}^2 - r_1{}^2\ (2\ln(r_1) +1)\,) - B_2\ (2\ r_0{}^2\ln(r_0) - r_0{}^2\ (2\ln(r_1) -1) - r_1{}^2)\ r_1{}^2] - c_{12}[\, B_1\, r_0{}^2(2\ln(r_0)\, r_1{}^2 - r_0{}^2 - r_1{}^2\ (2\ln(r_1) - 1)\,) - B_2\ (2\ r_0{}^2\ln(r_0) - r_0{}^2\ (2\ln(r_1) +1) + r_1{}^2)\ r_1{}^2]\,\} / [2\ (r_0{}^2 - r_1{}^2)\,] - (f_{12}\frac{\partial \overline{u_f}}{\partial z} + B_1\ (f_{12} + f_{12}))$

L. $(\overline{\sigma_{r_c}} - \overline{\sigma_{r_f}})$ **in term of** B_1, B_2, A_1, **and** A_2

$\overline{\sigma_{r}}_{m} - 2\overline{\sigma_{r}}_{c} = -\frac{1}{\frac{(r_2{}^2-r_1{}^2)}{2}}\{\, m_{12}\ (r_1{}^2 - r_2{}^2)^2\ \frac{\partial \overline{u_m}}{\partial z} + [\, m_{22}(2\ln(r_1)\, r_2{}^2 + r_1{}^2 - r_2{}^2\ (2\ln(r_2) +1)\,) - m_{12}\ (2\ln(r_1)\, r_2{}^2 - r_1{}^2 - r_2{}^2\ (2\ln(r_2) - 1)\,)\,]\, B_2\, r_1{}^2\,\} / [2\ (r_1{}^2 - r_2{}^2)\,] + \frac{2}{\frac{(r_1{}^2-r_0{}^2)}{2}}\{\, c_{12}\ (r_0{}^2 - r_1{}^2)^2\ \frac{\partial \overline{u_c}}{\partial z} + c_{22}[\, B_1\, r_0{}^2(2\ln(r_0)\, r_1{}^2 + r_0{}^2 - r_1{}^2\ (2\ln(r_1) +1)\,) - B_2\ (2\ r_0{}^2\ln(r_0) - r_0{}^2\ (2\ln(r_1) -1) - r_1{}^2)\ r_1{}^2] - c_{12}[\, B_1\, r_0{}^2(2\ln(r_0)\, r_1{}^2 - r_0{}^2 - r_1{}^2\ (2\ln(r_1) - 1)\,) - B_2\ (2\ r_0{}^2\ln(r_0) - r_0{}^2\ (2\ln(r_1) +1) + r_1{}^2)\ r_1{}^2]\,\} / [2\ (r_0{}^2 - r_1{}^2)\,]$

M. Getting the last two composite system equations by eliminating the averaged stresses variables $\overline{\sigma_{rf}}$, $\overline{\sigma_{rc}}$, and $\overline{\sigma_{rm}}$

Eliminate the averaged stresses variables form equations (47), (79), (56), and (57) to get:

$$\frac{r_0^2}{4}\left(\frac{\partial^2 B_1}{\partial t^2}\rho_c - \frac{\partial A_1}{\partial z}\right) + \left[\frac{\partial A_1}{\partial z} r_0^2\left[2\ln(r_0^2)\,r_1^4 + r_0^4 - 4\,r_0^2 r_1^2 - r_1^4\,(2\ln(r_1^2)-3)\right] - \frac{\partial A_2}{\partial z}\left[2\,r_0^2\ln(r_0^2)\,r_1^2 - r_0^4 - 2\,r_0^2 r_1^2\ln(r_1^2) + r_1^4\right] r_1^2 - \frac{\partial^2 B_1}{\partial t^2}\rho_c\, r_0^2\left[2\ln(r_0^2)\,r_1^4 + r_0^4 - 4\,r_0^2 r_1^2 - r_1^4\,(2\ln(r_1^2)-3)\right] + \frac{\partial^2 B_2}{\partial t^2}\rho_c\left[2\,r_0^2\ln(r_0^2)\,r_1^2 - r_0^4 - 4\,r_0^2 r_1^2\ln(r_1^2) + r_1^4\right] r_1^2 + 8\,(B_1 - B_2)\,c_{55}\left[r_0^2\ln(r_0^2) - r_0^2[\ln(r_1^2)+1] + r_1^2\right]\right] / \left[4\,(r_0^2 - r_1^2)^2\right] =$$

$$-\frac{1}{\frac{(r_1^2 - r_0^2)}{2}}\Big\{ c_{12}\,(r_0^2 - r_1^2)^2\frac{\partial \overline{u_c}}{\partial z} + c_{22}\big[B_1\, r_0^2(2\ln(r_0)\,r_1^2 + r_0^2 - r_1^2\,(2\ln(r_1)+1)) - B_2\,(2\,r_0^2\ln(r_0) - r_0^2\,(2\ln(r_1)-1) - r_1^2)\,r_1^2\big] - c_{12}\big[B_1\, r_0^2(2\ln(r_0)\,r_1^2 - r_0^2 - r_1^2\,(2\ln(r_1)-1)) - B_2\,(2\,r_0^2\ln(r_0) - r_0^2\,(2\ln(r_1)+1) + r_1^2)\,r_1^2\big]\Big\} / \left[2\,(r_0^2 - r_1^2)\right] - \left(f_{12}\frac{\partial \overline{u_f}}{\partial z} + B_1\,(f_{12} + f_{12})\right)$$

Also,

- [$\frac{\partial A_1}{\partial z}$ $r_0{}^2$ [2 ln($r_0{}^2$) $r_1{}^4$ + $r_0{}^4$ - 4 $r_0{}^2$ $r_1{}^2$ - $r_1{}^4$ (2 ln($r_1{}^2$)-3)] - $\frac{\partial A_2}{\partial z}$ [2 $r_0{}^2$ ln($r_0{}^2$) $r_1{}^2$ - $r_0{}^4$ - 2 $r_0{}^2$ $r_1{}^2$ ln($r_1{}^2$) + $r_1{}^4$] $r_1{}^2$- $\frac{\partial^2 B_1}{\partial t^2}$ ρ_c $r_0{}^2$ [2 ln($r_0{}^2$) $r_1{}^4$ + $r_0{}^4$ - 4 $r_0{}^2$ $r_1{}^2$ - $r_1{}^4$ (2 ln($r_1{}^2$)-3)] + $\frac{\partial^2 B_2}{\partial t^2}$ ρ_c [2 $r_0{}^2$ ln($r_0{}^2$) $r_1{}^2$ - $r_0{}^4$ - 4 $r_0{}^2$ $r_1{}^2$ ln($r_1{}^2$) + $r_1{}^4$] $r_1{}^2$ + 8 ($B_1 - B_2$) c_{55} [$r_0{}^2$ ln($r_0{}^2$) $- r_0{}^2$[ln($r_1{}^2$) + 1] + $r_1{}^2$]] / [4 ($r_0{}^2 - r_1{}^2$) ^{2}] + [$\frac{\partial A_2}{\partial z}$ $r_1{}^2$ [2 ln($r_1{}^2$) $r_2{}^4$ + $r_1{}^4$ - 4 $r_1{}^2$ $r_2{}^2$ - $r_2{}^4$ (2 ln($r_2{}^2$)-3)] - $\frac{\partial^2 B_2}{\partial t^2}$ $r_1{}^2$ ρ_m [2 ln($r_1{}^2$) $r_2{}^4$ -$r_1{}^4$ - 4 $r_1{}^2$ $r_2{}^2 -$ $r_2{}^4$ [2 ln($r_2{}^2$) -3]]+ 8 (B_2) m_{55} [$r_1{}^2$ ln($r_1{}^2$) $- r_1{}^2$[ln($r_2{}^2$) + 1] + $r_2{}^2$] $r_2{}^2$] / [4 ($r_1{}^2 - r_2{}^2$) ^{2}] = $-\frac{1}{\frac{(r_2{}^2-r_1{}^2)}{2}}$ { m_{12} ($r_1{}^2 - r_2{}^2$)^2 $\frac{\partial \overline{u_m}}{\partial z}$ + [m_{22}(2 ln(r_1) $r_2{}^2$ + $r_1{}^2$ - $r_2{}^2$ (2 ln(r_2) +1)) $- m_{12}$ (2 ln(r_1) $r_2{}^2$ - $r_1{}^2$ - $r_2{}^2$ (2 ln(r_2) - 1))] B_2 $r_1{}^2$ } / [2 ($r_1{}^2 - r_2{}^2$)] + $\frac{2}{\frac{(r_1{}^2-r_0{}^2)}{2}}$ { c_{12} ($r_0{}^2 - r_1{}^2$)^2 $\frac{\partial \overline{u_c}}{\partial z}$ + c_{22}[B_1 $r_0{}^2$(2 ln(r_0) $r_1{}^2$ + $r_0{}^2$ - $r_1{}^2$ (2 ln(r_1) +1)) $- B_2$ (2 $r_0{}^2$ ln(r_0) - $r_0{}^2$ (2 ln(r_1) -1) $- r_1{}^2$) $r_1{}^2$] $- c_{12}$[B_1 $r_0{}^2$(2 ln(r_0) $r_1{}^2$ - $r_0{}^2$ - $r_1{}^2$ (2 ln(r_1) - 1)) $- B_2$ (2 $r_0{}^2$ ln(r_0) - $r_0{}^2$ (2 ln(r_1) +1) + $r_1{}^2$) $r_1{}^2$] } / [2 ($r_0{}^2 - r_1{}^2$)]

Now, these two long equations need be simplified

First, starting with equation (58) by letting:

$\Omega_0 = \frac{1}{\frac{(r_1{}^2-r_0{}^2)}{2}}$ Cc_{12} ($r_0{}^2 - r_1{}^2$)^2 / [2($r_0{}^2 - r_1{}^2$)^2]

Ω_1= $r_0{}^2$ [2 ln($r_0{}^2$) $r_1{}^4$ + $r_0{}^4$ - 4 $r_0{}^2$ $r_1{}^2$ - $r_1{}^4$ (2 ln($r_1{}^2$)-3)] / [4 ($r_0{}^2 - r_1{}^2$) ^{2}]

Ω_2= $[2\, r_0^{\,2}\, \ln(r_0^{\,2})\, r_1^{\,2} - r_0^{\,4} - 2\, r_0^{\,2}\, r_1^{\,2}\, \ln(r_1^{\,2}) + r_1^{\,4}]\, r_1^{\,2} \,/\, [4\,(r_0^{\,2} - r_1^{\,2}\,)^{\,2}\,]$

Ω_3= $\rho_c\, r_0^{\,2}\, [2\, \ln(r_0^{\,2})\, r_1^{\,4} + r_0^{\,4} - 4\, r_0^{\,2}\, r_1^{\,2} - r_1^{\,4}\,(2\, \ln(r_1^{\,2})\text{-}3)\,] \,/\, [4\,(r_0^{\,2} - r_1^{\,2}\,)^{\,2}\,]$

Ω_4= $\rho_c\, [2\, r_0^{\,2}\, \ln(r_0^{\,2})\, r_1^{\,2} - r_0^{\,4} - 4\, r_0^{\,2}\, r_1^{\,2}\, \ln(r_1^{\,2}) + r_1^{\,4}]\, r_1^{\,2} / [4\,(r_0^{\,2} - r_1^{\,2}\,)^{\,2}\,]$

Ω_5=$[8\, c_{55}\, [r_0^{\,2}\, \ln(r_0^{\,2}) - r_0^{\,2}[\, \ln(r_1^{\,2}) + 1] + r_1^{\,2}] \,/\, [4\,(r_0^{\,2} - r_1^{\,2}\,)^{\,2}\,]$

Ω_6= $\frac{1}{\frac{(r_1^{\,2} - r_0^{\,2})}{2}}\; c_{22} r_0^{\,2} (2\, \ln(r_0)\, r_1^{\,2} + r_0^{\,2} - r_1^{\,2}\, (\,2\, \ln(r_1) + 1)\,) \,/\, [2\,(r_0^{\,2} - r_1^{\,2})\,]$

Ω_7= $\frac{1}{\frac{(r_1^{\,2} - r_0^{\,2})}{2}}\; c_{22}\, (2\, r_0^{\,2}\, \ln(r_0) - r_0^{\,2}\, (\,2\, \ln(r_1) - 1) - r_1^{\,2})\;\; r_1^{\,2} \,/\, [2\,(r_0^{\,2} - r_1^{\,2})\,]$

Ω_8= $\frac{1}{\frac{(r_1^{\,2} - r_0^{\,2})}{2}}\; c_{12}\, r_0^{\,2} (2\, \ln(r_0)\, r_1^{\,2} - r_0^{\,2} - r_1^{\,2}\, (\,2\, \ln(r_1) - 1)\,) \,/\, [2\,(r_0^{\,2} - r_1^{\,2})\,]$

Ω_9= $\frac{1}{\frac{(r_1^{\,2} - r_0^{\,2})}{2}}\; c_{12}\, (2\, r_0^{\,2}\, \ln(r_0) - r_0^{\,2}\, (\,2\, \ln(r_1) + 1) + r_1^{\,2})\;\; r_1^{\,2} \,/\, [2\,(r_0^{\,2} - r_1^{\,2})\,]$

As a result, equation (58) will be simplified to:

$$\frac{r_0^{\,2}}{4}\, \frac{\partial^2 B_1}{\partial t^2}\, \rho_c - \frac{r_0^{\,2}}{4}\, \frac{\partial A_1}{\partial z} + \Omega_1\, \frac{\partial A_1}{\partial z} - \Omega_2\, \frac{\partial A_2}{\partial z} - \Omega_3\, \frac{\partial^2 B_1}{\partial t^2} + \Omega_4\, \frac{\partial^2 B_2}{\partial t^2} + \Omega_5\, B_1 - \Omega_5\, B_2 = -$$

$$\Omega_0\, \frac{\partial \overline{u_c}}{\partial z} - \Omega_6\, B_1 + B_2 \Omega_7 + \Omega_8\, B_1 - \Omega_9\, B_2 - f_{12}\, \frac{\partial \overline{u_f}}{\partial z} - B_1\,(f_{12} + f_{12})$$

Finally, equation (59) is going to be simplified by letting:

¥$_0$= $r_0{}^2$ [2 $\ln(r_0{}^2)$ $r_1{}^4$ + $r_0{}^4$ - 4 $r_0{}^2$ $r_1{}^2$ - $r_1{}^4$ (2 $\ln(r_1{}^2)$-3) / [4 $(r_0{}^2 - r_1{}^2)^2$]

¥$_1$= [2 $r_0{}^2$ $\ln(r_0{}^2)$ $r_1{}^2$ - $r_0{}^4$ - 2 $r_0{}^2$ $r_1{}^2$ $\ln(r_1{}^2)$ + $r_1{}^4$] $r_1{}^2$/ [4 $(r_0{}^2 - r_1{}^2)^2$]

¥$_2$= ρ_c $r_0{}^2$ [2 $\ln(r_0{}^2)$ $r_1{}^4$ + $r_0{}^4$ - 4 $r_0{}^2$ $r_1{}^2$ - $r_1{}^4$ (2 $\ln(r_1{}^2)$-3)] / [4 $(r_0{}^2 - r_1{}^2)^2$]

¥$_3$= ρ_c [2 $r_0{}^2$ $\ln(r_0{}^2)$ $r_1{}^2$ - $r_0{}^4$ - 4 $r_0{}^2$ $r_1{}^2$ $\ln(r_1{}^2)$ + $r_1{}^4$] $r_1{}^2$ / [4 $(r_0{}^2 - r_1{}^2)^2$]

¥$_4$= 8 c_{44} [$r_0{}^2 \ln(r_0{}^2) - r_0{}^2[\ln(r_1{}^2) + 1] + r_1{}^2$] / [4 $(r_0{}^2 - r_1{}^2)^2$]

¥$_5$= $r_1{}^2$ [2 $\ln(r_1{}^2)$ $r_2{}^4$ + $r_1{}^4$ - 4 $r_1{}^2$ $r_2{}^2$ - $r_2{}^4$ (2 $\ln(r_2{}^2)$-3) / [4 $(r_1{}^2 - r_2{}^2)^2$]

¥$_6$= $r_1{}^2$ ρ_m [2 $\ln(r_1{}^2)$ $r_2{}^4$ -$r_1{}^4$ - 4 $r_1{}^2$ $r_2{}^2$ $-$ $r_2{}^4$ [2 $\ln(r_2{}^2)$ – 3]] / [4 $(r_1{}^2 - r_2{}^2)^2$]

¥$_7$= 8 m_{44} [$r_1{}^2 \ln(r_1{}^2) - r_1{}^2[\ln(r_2{}^2) + 1] + r_2{}^2$] $r_2{}^2$] / [4 $(r_1{}^2 - r_2{}^2)^2$]

¥$_8$= $\frac{1}{\frac{(r_2{}^2 - r_1{}^2)}{2}}$ m_{12} $(r_1{}^2 - r_2{}^2)^2$ / [2 $(r_1{}^2 - r_2{}^2)$]

¥$_9$= $\frac{1}{\frac{(r_2{}^2 - r_1{}^2)}{2}}$ [m_{22}(2 $\ln(r_1)$ $r_2{}^2$ + $r_1{}^2$ - $r_2{}^2$ (2 $\ln(r_2)$ +1)) $-$ m_{12} (2 $\ln(r_1)$ $r_2{}^2$ - $r_1{}^2$ -

$r_2{}^2$ (2 $\ln(r_2)$ - 1))] $r_1{}^2$ / [2 $(r_1{}^2 - r_2{}^2)$]

¥$_{10}$= $\frac{2}{\frac{(r_1{}^2 - r_0{}^2)}{2}}$ CNT_{12} $(r_0{}^2 - r_1{}^2)^2$ / [2 $(r_0{}^2 - r_1{}^2)$]

$$\yen_{11}= \frac{2}{\frac{(r_1{}^2-r_0{}^2)}{2}}\ c_{22}[\ r_0{}^2(2\ \ln(r_0)\ r_1{}^2 + r_0{}^2 -\ r_1{}^2\ \ (\ 2\ \ln(r_1)\ +1)\ )]\ /\ [2\ (r_0{}^2 - r_1{}^2)\ ]$$

$$\yen_{12}= \frac{2}{\frac{(r_1{}^2-r_0{}^2)}{2}}\ c_{22}[\ (2\ \ r_0{}^2\ \ln(r_0) - r_0{}^2\ \ (\ 2\ \ln(r_1)\ -1) -\ \ r_1{}^2)\ \ r_1{}^2]\ /\ [2\ (r_0{}^2 - r_1{}^2)\ ]$$

$$\yen_{13}= \frac{2}{\frac{(r_1{}^2-r_0{}^2)}{2}}\ c_{12}[\ \ r_0{}^2(2\ \ln(r_0)\ r_1{}^2 - r_0{}^2 -\ r_1{}^2\ \ (\ 2\ \ln(r_1)\ -\ 1)\ )]\ /\ [2\ (r_0{}^2 - r_1{}^2)\ ]$$

$$\yen_{14}= \frac{2}{\frac{(r_1{}^2-r_0{}^2)}{2}}\ c_{12}[\ \ (2\ \ r_0{}^2\ \ln(r_0) - r_0{}^2\ \ (\ 2\ \ln(r_1)\ +1) +\ \ r_1{}^2)\ \ r_1{}^2]\ \ /\ [2\ (r_0{}^2 - r_1{}^2)\ ]$$

Therefore, equation (59) is going to be simplified as:

$$- \yen_0 \frac{\partial A_1}{\partial z} + \ \yen_1 \frac{\partial A_2}{\partial z}\ + \frac{\partial^2 B_1}{\partial t^2}\ \yen_2 - \frac{\partial^2 B_2}{\partial t^2}\ \yen_3 - B_1\ \yen_4 + B_2\ \yen_4 + \ \yen_5 \frac{\partial A_2}{\partial z}\ -\ \frac{\partial^2 B_2}{\partial t^2}\ \ \yen_6 +$$

$$B_2\ \yen_7 = - \yen_8 \frac{\partial \overline{u_m}}{\partial z}\ -\ \yen_9\ B_2 + \yen_{10}\ \frac{\partial \overline{u_c}}{\partial z} + \yen_{11}\ B_1 - \yen_{12}\ B_2 - \yen_{13}\ B_1 + \yen_{14}\ B_2$$

N. Relation of radial stress versus the composite radius for embedded cnt composite with air filling

```
r0=2*10^-9;
r1=2.34*10^-9;
r2=8.34*10^-9;
o1=2*45*10^9;
o2=4*45*10^9;

nf=r0^2/r2^2;
nc=(r1^2-r0^2)/r2^2;
nm=(r2^2-r1^2)/r2^2;
B1=o1/r0;
B2=o2/r1;

r=r1:r2/25:r2;
i=length(r);
om=(B2*((nc+nf)/nm)*((r2./r).^2-1).*r);
subplot(1, 3, 3)
plot(r,om,'r')
xlabel('rm');
ylabel('om');
grid

r=0:r0/25:r0;
i=length(r);
of=B1.*r;
subplot(1, 3, 1)
plot(r,of,'r')
xlabel('rf');
ylabel('of');
grid

r=r0:r1/25:r1;
```

```
i=length(r);
oc=(s1*(nf/nc)*((r1./r).^2-1).*r)-(B2*((1-nm)/nc)*((r0./r).^2-1).*r);
subplot(1, 3, 2)
plot(r,oc,'r')
xlabel('rc');
ylabel('oc');
grid
```

O. MatLab programming for embedded cnt fibrous composite solution

```
digits (2)
syms c w
r0     = "inter the value of r0";
r1     = "inter the value of r1"
r2     = "inter the value of r2";
E=1.12*10^12;
v=.3;
c12= (v*E)/(1-v^2);
c11= E/(1-v^2);
c44= E/(2*(1+v^2));
nc     = (r1^2-r0^2)/r2^2;
rho_c  = 1700;
f11    = 0;
f12    = 0;
f22    = 0;
f55    =0;
nf     = (r0^2)/r2^2;
rho_f  = 1.2;
m11    = 193*10^9;
m12    = 103*10^9;
m44    = 45*10^9;
m55    = 45*10^9;
m22    = 45*10^9;
```

```
rho_m   = 3200;
nm      = (r2^2-r1^2)/r2^2;

 z0=cnt55*r0^2*(4*log10(r0)*r1^4+r0^4-4*r0^2*r1^2-r1^4*(4*log10(r1)-
3))/(4*cnt55*(r0^2-r1^2)^2);
 z1=cnt55*(4*r0^2*log10(r0)*r1^2-r0^4-
4*r0^2*r1^2*log10(r1)+r1^4)*r1^2/(4*cnt55*(r0^2-r1^2)^2);
 z2=r0^2*(4*log10(r0)*r1^4+r0^4-4*r0^2*r1^2-r1^4*(4*log10(r1)-3))/(4*cnt55*(r0^2-
r1^2)^2);
 z3=(4*r0^2*log10(r0)*r1^2-r0^4-4*r0^2*r1^2*log10(r1)+r1^4)*r1^2/(4*cnt55*(r0^2-
r1^2)^2);
 z4=r0^2/4;
 z5=cnt55*r0^2*(4*log10(r0)*r1^4+r0^4-4*r0^2*r1^2-r1^4*(4*log10(r1)-
3))/(4*cnt55*(r0^2-r1^2)^2);
 z6=cnt55*(4*r0^2*log10(r0)*r1^2-r0^4-
4*r0^2*r1^2*log10(r1)+r1^4)*r1^2/(4*cnt55*(r0^2-r1^2)^2);
 z7=r0^2*(4*log10(r0)*r1^4+r0^4-4*r0^2*r1^2-r1^4*(4*log10(r1)-3))/(4*cnt55*(r0^2-
r1^2)^2);
 z8=(4*r0^2*log10(r0)*r1^2-r0^4-4*r0^2*r1^2*log10(r1)+r1^4)*r1^2/(4*cnt55*(r0^2-
r1^2)^2);
 z9=r1^2*(4*log10(r1)*r2^4+r1^4-4*r1^2*r2^2-r2^4*(4*log10(r2)-3))/(4*cnt55*(r1^2-
r2^2)^2);

 g0=1/((r1^2-r0^2)/2)*cnt12*(r0^2-r1^2)^2/(2*(r0^2-r1^2));
 g1=r0^2*(2*log10(r0^2)*r1^4+r0^4-4*r0^2*r1^2-r1^4*(2*log10(r1^2)-3))/(4*(r0^2-
r1^2)^2);
 g2=(2*r0^2*log10(r0^2)*r1^2-r0^4-2*r0^2*r1^2*log10(r1^2)+r1^4)*r1^2/(4*(r0^2-
r1^2)^2);
 g3=rho_c*r0^2*(2*log10(r0^2)*r1^4+r0^4-4*r0^2*r1^2-r1^4*(2*log10(r1^2)-
3))/(4*(r0^2-r1^2)^2);
 g4=rho_c*(2*r0^2*log10(r0^2)*r1^2-r0^4-
4*r0^2*r1^2*log10(r1^2)+r1^4)*r1^2/(4*(r0^2-r1^2)^2);
 g5=8*cnt55*(r0^2*log10(r0^2)-r0^2*(log10(r1^2)+1)+r1^2)/(4*(r0^2-r1^2)^2);
```

```
g6=1/((r1^2-r0^2)/2)*cnt22*r0^2*(2*log10(r0)*r1^2+r0^2-
r1^2*(2*log10(r1)+1))/(2*(r0^2-r1^2));
g7=1/((r1^2-r0^2)/2)*cnt22*(2*r0^2*log10(r0)-r0^2*(2*log10(r1)-1)-
r1^2)*r1^2/(2*(r0^2-r1^2));
g8=1/((r1^2-r0^2)/2)*cnt12*r0^2*(2*log10(r0)*r1^2-r0^2-r1^2*(2*log10(r1)-
1))/(2*(r0^2-r1^2));
g0=1/((r1^2-r0^2)/2)*cnt12*(r0^2-r1^2)^2/(2*(r0^2-r1^2));
g6=1/((r1^2-r0^2)/2)*cnt22*r0^2*(2*log10(r0)*r1^2+r0^2-
r1^2*(2*log10(r1)+1))/(2*(r0^2-r1^2));
g7=1/((r1^2-r0^2)/2)*cnt22*(2*r0^2*log10(r0)-r0^2*(2*log10(r1)-1)-
r1^2)*r1^2/(2*(r0^2-r1^2));
g9=1/((r1^2-r0^2)/2)*cnt12*(2*r0^2*log10(r0)-
r0^2*(2*log10(r1)+1)+r1^2)*r1^2/(2*(r0^2-r1^2));

y0=r0^2*(2*log10(r0^2)*r1^4+r0^4-4*r0^2*r1^2-r1^4*(2*log10(r1^2)-3))/(4*(r0^2-
r1^2)^2);
y1=(2*r0^2*log10(r0^2)*r1^2-r0^4-2*r0^2*r1^2*log10(r1^2)+r1^4)*r1^2/(4*(r0^2-
r1^2)^2);
y2=rho_c*r0^2*(2*log10(r0^2)*r1^4+r0^4-4*r0^2*r1^2-r1^4*(2*log10(r1^2)-
3))/(4*(r0^2-r1^2)^2);
y3=rho_c*(2*r0^2*log10(r0^2)*r1^2-r0^4-
4*r0^2*r1^2*log10(r1^2)+r1^4)*r1^2/(4*(r0^2-r1^2)^2);
y4=8*cnt55*(r0^2*log10(r0^2)-r0^2*(log10(r1^2)+1)+r1^2)/(4*(r0^2-r1^2)^2);
y5=r1^2*(2*log10(r1^2)*r2^4+r1^4-4*r1^2*r2^2-r2^4*(2*log10(r2^2)-3))/(4*(r1^2-
r2^2)^2);
y6=rho_m*r1^2*(2*log10(r1^2)*r2^4-r1^4-4*r1^2*r2^2-r2^4*(2*log10(r2^2)-
3))/(4*(r1^2-r2^2)^2);
y7=8*m44*(r1^2*log10(r1^2)-r1^2*(log10(r2^2)+1)+r2^2)*r2^2/(4*(r1^2-r2^2)^2);
y8=1/((r2^2-r1^2)/2)*m12*(r1^2-r2^2)^2/(2*(r1^2-r2^2));
y9=1/((r2^2-r1^2)/2)*(m22*(2*r2^2*log10(r1)+r1^2-r2^2*(2*log10(r2)+1))-
m12*(2*r2^2*log10(r1)-r1^2-r2^2*(2*log10(r2)-1)))*r1^2/(2*(r1^2-r2^2));
y10=2/((r1^2-r0^2)/2)*cnt12*(r0^2-r1^2)^2/(2*(r0^2-r1^2));
y11=2/((r1^2-r0^2)/2)*cnt22*(r0^2*(2*log10(r0)*r1^2+r0^2-
r1^2*(2*log10(r1)+1)))/(2*(r0^2-r1^2));
```

```
y12=2/((r1^2-r0^2)/2)*cnt22*((2*r0^2*log10(r0)-r0^2*(2*log10(r1)-1)-
r1^2)*r1^2)/(2*(r0^2-r1^2));
y13=2/((r1^2-r0^2)/2)*cnt12*(r0^2*(2*log10(r0)*r1^2-r0^2-r1^2*(2*log10(r1)-
1)))/(2*(r0^2-r1^2));
y14=2/((r1^2-r0^2)/2)*cnt12*((2*r0^2*log10(r0)-
r0^2*(2*log10(r1)+1)+r1^2)*r1^2)/(2*(r0^2-r1^2));


A      = [nf*(rho_f*c^2-f11)     0                    0                   2*nf/(w/c)^2
0                  2*nf*f12/(w/c)                    0
      0                  nc*(rho_c*c^2-cnt11)        0                  -2*nf/(w/c)^2
2*(nf+nc)/(w/c)^2                                   -4*cnt12*(nf+nc)*nf/(w/c)
2*cnt12*(nf+nc)/(w/c)
      0                  0                    nm*(rho_m*c^2-m11)        0
-2*(nf+nc)/(w/c)^2         0                   -2*m12*(nf+nc)/(w/c)
      1/(w/c)^2             -1/(w/c)^2               0                  (-z2)/(w/c)^2
z3/(w/c)^2              (z0-z4)/(w/c)                     -z1/(w/c)
      0                  2/(w/c)^2              -1/(w/c)^2              z7/(w/c)^2
-(z8+z9)/(w/c)^2           -z5/(w/c)                    (z8+m55*z9)/(w/c)
      -f12/(w/c)            -g0/(w/c)                 0                   (r0^2/4-
g1)/(w/c)               g2/(w/c)                    (g8-g6-g5-2*f12)/(w/c)^2-(-
rho_c*r0^2/4+g2)*c^2      (g7-g9+g5)/(w/c)^2+g4*c^2
      0                  y10/(w/c)               -y5/(w/c)                y0/(w/c)
-(y1+y5)/(w/c)          (y4+y11-y13)/(w/c)^2+y2*c^2                       (y14-y9-
y12-y7-y4)/(w/c)^2-(y8+y3)*c^2];

d = det(A);
dd=vpa (d);
solve (dd,w);
a=solve (dd,w);
stp = 10^6/2;
w = 0:stp:100*10^5;
a1 = simplify(a);
a = solve(d,c);  % solve d = 0 to find c in terms of w
```

```
a1 = simplify(a);

h1 = figure,grid
for p = 1:2
   hold on
   a1p = a1(p,:);
   a1ps = subs(a1p,w);
   plot(w,a1ps,'r')
end
xlabel('w'), ylabel('c')
print -djpeg fig1
print -dbmp  fig1

h2 = figure,grid
for p = 3:4
   hold on
   a1p = a1(p,:);
   a1ps = subs(a1p,w);
   plot(w,a1ps,'g')
end
xlabel('w'), ylabel('c')

print -djpeg fig2
print -dbmp fig2
h = figure,grid
for p = 5:6
   hold on
   a1p = a1(p,:);
   a1ps = subs(a1p,w);
   plot(w,a1ps,'b')
end
xlabel('w'), ylabel('c')

print -djpeg fig3
print -dbmp fig3
%%
% A1 = subs(a1,w);
%
% R1 = real(A1);
% I1 = imag(A1);
%
% %% Plots
% figure,
% for p =1:6
%     hold on
%     plot(k,R1(p,:))
% end
% grid
```

P. MatLab programming for fibrous composite solutions

//since the filling radius equal zero in this case, the fiber will be represented in the program as "cnt"

```
digits (2)
syms c w
r0     = 0
r1     = "inter the value of r1"
r2     = "inter the value of r2";
cnt11    = 381.3*10^9;
cnt12    = 58.24 *10^9;
cnt22    = 37.29*10^9;
cnt44    = 262.8*10^9;
cnt55    = 65.35 *10^9;
nc     = (r1^2-r0^2)/r2^2;
rho_c   = 1700;
f11    = 0;
f12    = 0;
f22    = 0;
f55    =0;
nf     = (r0^2)/r2^2;
rho_f   = 1.2;
m11    = 193*10^9;
m12    = 103*10^9;
m44    = 45*10^9;
m55    = 45*10^9;
m22    = 45*10^9;
rho_m   = 3200;
nm     = (r2^2-r1^2)/r2^2;

z0=cnt55*r0^2*(4*log10(r0)*r1^4+r0^4-4*r0^2*r1^2-r1^4*(4*log10(r1)-
3))/(4*cnt55*(r0^2-r1^2)^2);
```

```
z1=cnt55*(4*r0^2*log10(r0)*r1^2-r0^4-
4*r0^2*r1^2*log10(r1)+r1^4)*r1^2/(4*cnt55*(r0^2-r1^2)^2);
z2=r0^2*(4*log10(r0)*r1^4+r0^4-4*r0^2*r1^2-r1^4*(4*log10(r1)-3))/(4*cnt55*(r0^2-
r1^2)^2);
z3=(4*r0^2*log10(r0)*r1^2-r0^4-4*r0^2*r1^2*log10(r1)+r1^4)*r1^2/(4*cnt55*(r0^2-
r1^2)^2);
z4=r0^2/4;
z5=cnt55*r0^2*(4*log10(r0)*r1^4+r0^4-4*r0^2*r1^2-r1^4*(4*log10(r1)-
3))/(4*cnt55*(r0^2-r1^2)^2);
z6=cnt55*(4*r0^2*log10(r0)*r1^2-r0^4-
4*r0^2*r1^2*log10(r1)+r1^4)*r1^2/(4*cnt55*(r0^2-r1^2)^2);
z7=r0^2*(4*log10(r0)*r1^4+r0^4-4*r0^2*r1^2-r1^4*(4*log10(r1)-3))/(4*cnt55*(r0^2-
r1^2)^2);
z8=(4*r0^2*log10(r0)*r1^2-r0^4-4*r0^2*r1^2*log10(r1)+r1^4)*r1^2/(4*cnt55*(r0^2-
r1^2)^2);
z9=r1^2*(4*log10(r1)*r2^4+r1^4-4*r1^2*r2^2-r2^4*(4*log10(r2)-3))/(4*cnt55*(r1^2-
r2^2)^2);

g0=1/((r1^2-r0^2)/2)*cnt12*(r0^2-r1^2)^2/(2*(r0^2-r1^2));
g1=r0^2*(2*log10(r0^2)*r1^4+r0^4-4*r0^2*r1^2-r1^4*(2*log10(r1^2)-3))/(4*(r0^2-
r1^2)^2);
g2=(2*r0^2*log10(r0^2)*r1^2-r0^4-2*r0^2*r1^2*log10(r1^2)+r1^4)*r1^2/(4*(r0^2-
r1^2)^2);
g3=rho_c*r0^2*(2*log10(r0^2)*r1^4+r0^4-4*r0^2*r1^2-r1^4*(2*log10(r1^2)-
3))/(4*(r0^2-r1^2)^2);
g4=rho_c*(2*r0^2*log10(r0^2)*r1^2-r0^4-
4*r0^2*r1^2*log10(r1^2)+r1^4)*r1^2/(4*(r0^2-r1^2)^2);
g5=8*cnt55*(r0^2*log10(r0^2)-r0^2*(log10(r1^2)+1)+r1^2)/(4*(r0^2-r1^2)^2);
g6=1/((r1^2-r0^2)/2)*cnt22*r0^2*(2*log10(r0)*r1^2+r0^2-
r1^2*(2*log10(r1)+1))/(2*(r0^2-r1^2));
g7=1/((r1^2-r0^2)/2)*cnt22*(2*r0^2*log10(r0)-r0^2*(2*log10(r1)-1)-
r1^2)*r1^2/(2*(r0^2-r1^2));
g8=1/((r1^2-r0^2)/2)*cnt12*r0^2*(2*log10(r0)*r1^2-r0^2-r1^2*(2*log10(r1)-
1))/(2*(r0^2-r1^2));
```

```
g0=1/((r1^2-r0^2)/2)*cnt12*(r0^2-r1^2)^2/(2*(r0^2-r1^2));
g6=1/((r1^2-r0^2)/2)*cnt22*r0^2*(2*log10(r0)*r1^2+r0^2-
r1^2*(2*log10(r1)+1))/(2*(r0^2-r1^2));
g7=1/((r1^2-r0^2)/2)*cnt22*(2*r0^2*log10(r0)-r0^2*(2*log10(r1)-1)-
r1^2)*r1^2/(2*(r0^2-r1^2));
g9=1/((r1^2-r0^2)/2)*cnt12*(2*r0^2*log10(r0)-
r0^2*(2*log10(r1)+1)+r1^2)*r1^2/(2*(r0^2-r1^2));

y0=r0^2*(2*log10(r0^2)*r1^4+r0^4-4*r0^2*r1^2-r1^4*(2*log10(r1^2)-3))/(4*(r0^2-
r1^2)^2);
y1=(2*r0^2*log10(r0^2)*r1^2-r0^4-2*r0^2*r1^2*log10(r1^2)+r1^4)*r1^2/(4*(r0^2-
r1^2)^2);
y2=rho_c*r0^2*(2*log10(r0^2)*r1^4+r0^4-4*r0^2*r1^2-r1^4*(2*log10(r1^2)-
3))/(4*(r0^2-r1^2)^2);
y3=rho_c*(2*r0^2*log10(r0^2)*r1^2-r0^4-
4*r0^2*r1^2*log10(r1^2)+r1^4)*r1^2/(4*(r0^2-r1^2)^2);
y4=8*cnt55*(r0^2*log10(r0^2)-r0^2*(log10(r1^2)+1)+r1^2)/(4*(r0^2-r1^2)^2);
y5=r1^2*(2*log10(r1^2)*r2^4+r1^4-4*r1^2*r2^2-r2^4*(2*log10(r2^2)-3))/(4*(r1^2-
r2^2)^2);
y6=rho_m*r1^2*(2*log10(r1^2)*r2^4-r1^4-4*r1^2*r2^2-r2^4*(2*log10(r2^2)-
3))/(4*(r1^2-r2^2)^2);
y7=8*m44*(r1^2*log10(r1^2)-r1^2*(log10(r2^2)+1)+r2^2)*r2^2/(4*(r1^2-r2^2)^2);
y8=1/((r2^2-r1^2)/2)*m12*(r1^2-r2^2)^2/(2*(r1^2-r2^2));
y9=1/((r2^2-r1^2)/2)*(m22*(2*r2^2*log10(r1)+r1^2-r2^2*(2*log10(r2)+1))-
m12*(2*r2^2*log10(r1)-r1^2-r2^2*(2*log10(r2)-1)))*r1^2/(2*(r1^2-r2^2));
y10=2/((r1^2-r0^2)/2)*cnt12*(r0^2-r1^2)^2/(2*(r0^2-r1^2));
y11=2/((r1^2-r0^2)/2)*cnt22*(r0^2*(2*log10(r0)*r1^2+r0^2-
r1^2*(2*log10(r1)+1)))/(2*(r0^2-r1^2));
y12=2/((r1^2-r0^2)/2)*cnt22*((2*r0^2*log10(r0)-r0^2*(2*log10(r1)-1)-
r1^2)*r1^2)/(2*(r0^2-r1^2));
y13=2/((r1^2-r0^2)/2)*cnt12*(r0^2*(2*log10(r0)*r1^2-r0^2-r1^2*(2*log10(r1)-
1)))/(2*(r0^2-r1^2));
y14=2/((r1^2-r0^2)/2)*cnt12*((2*r0^2*log10(r0)-
r0^2*(2*log10(r1)+1)+r1^2)*r1^2)/(2*(r0^2-r1^2));
```

```
A      = [nf*(rho_f*c^2-f11)     0                    0                   2*nf/(w/c)^2
0                 2*nf*f12/(w/c)                      0
       0                 nc*(rho_c*c^2-cnt11)       0                  -2*nf/(w/c)^2
2*(nf+nc)/(w/c)^2                                           -4*cnt12*(nf+nc)*nf/(w/c)
2*cnt12*(nf+nc)/(w/c)
       0                   0                       nm*(rho_m*c^2-m11)      0
-2*(nf+nc)/(w/c)^2          0                             -2*m12*(nf+nc)/(w/c)
       1/(w/c)^2              -1/(w/c)^2                0               (-z2)/(w/c)^2
z3/(w/c)^2               (z0-z4)/(w/c)                           -z1/(w/c)
       0                 2/(w/c)^2                  -1/(w/c)^2              z7/(w/c)^2
-(z8+z9)/(w/c)^2              -z5/(w/c)                          (z8+m55*z9)/(w/c)
       -f12/(w/c)               -g0/(w/c)                     0                (r0^2/4-
g1)/(w/c)                g2/(w/c)                         (g8-g6-g5-2*f12)/(w/c)^2-(-
rho_c*r0^2/4+g2)*c^2         (g7-g9+g5)/(w/c)^2+g4*c^2
       0                 y10/(w/c)                  -y5/(w/c)                y0/(w/c)
-(y1+y5)/(w/c)              (y4+y11-y13)/(w/c)^2+y2*c^2                      (y14-y9-
y12-y7-y4)/(w/c)^2-(y8+y3)*c^2];

d = det(A);
dd=vpa (d);
solve (dd,w);
a=solve (dd,w);
stp = 10^6/2;
w = 0:stp:100*10^5;
a1 = simplify(a);
```

And for the graph of it, it will gives the same results if we use the following program:

```
r1="inter the value of r1"
r2="inter the value of r2"
syms c w
digits(4)
m44     = 45*10^3;
```

```
rho_m   = 3200;
f11     = 381.3*10^3;
f12     = 58.24*10^3;
m11     = 193*10^3;
m12     = 103*10^3;
eta_f   = r1^2/r2^2;
eta_m   = 1-eta_f;
rho_f   = 1700;
Q       = (1/eta_m^2)*(eta_f^2-4*eta_f+3+2*log10(eta_f));
zeta1   = 1/eta_m*(eta_m*(f11+f12)+eta_f*(m11+m12)+m44)
zeta2   = r1^2*(rho_f-Q*rho_m)/4;
f44     = 37.29*10^9;
eta2    = r1^2/4*(1/f44-Q/m44);
eta1    = r1^2/4*(1-Q);

A       = [eta_f*(rho_f*c^2-f11)    0                    2*eta_f/(w/c)^2     2*eta_f*f12/(w/c)
        0                    eta_m*(rho_m*c^2-m11)    -2*eta_f/(w/c)^2        -
2*eta_f*m12/(w/c)
        -1/(w/c)^2              1/(w/c)^2              -eta2/(w/c)^2        eta1/(w/c)
        -f12/(w/c)                  m12/(w/c)                      eta1/(w/c)            -
zeta1/(w/c)^2+zeta2*c^2];

d = det(A);
a = solve(d,c);


%%
stp = 10^6/8;
w = 1:stp:1*10^6;
a1 = simplify(a);
h1 = figure,grid
for p = 1:2
   hold on
   a1p = a1(p,:);
```

```
   a1ps = subs(a1p,w);
   plot(w,a1ps,'r')
end
xlabel('w'), ylabel('c')
print -djpeg fig1
print -dbmp  fig1

h2 = figure,grid
for p = 3:4
   hold on
   a1p = a1(p,:);
   a1ps = subs(a1p,w);
   plot(w,a1ps,'g')
end
xlabel('w'), ylabel('c')

print -djpeg fig2
print -dbmp fig2
h = figure,grid
for p = 5:6
   hold on
   a1p = a1(p,:);
   a1ps = subs(a1p,w);
   plot(w,a1ps,'b')
end
xlabel('w'), ylabel('c')
print -djpeg fig3
print -dbmp fig3
```

REFRENCES

[1] N Taniguchi. "**On the basic concept of 'Nano-Technology',**" Proc. Intl. Conf. Prod. London, Part II, British Society of Precision Engineering, 1974.

[2] L X Zheng et al. (2004). "**Ultralong single-wall carbon nanotubes**". 3. pp. 673–676

[3]**k"The invisible marvels of the nano worlds". http://www.lbl.gov/wonder/louie.html**. (Accessed 02/06/2008).

[4] F H Gojny, M H G Wichmann,U Kopke, B Fiedler, and K Schulte. "**Carbon nanotube-reinforced epoxy-composites: enhanced stiffness and fracture toughness at low nanotube content".** Sci Direct 2004:2363-2371.

[5] S Iijima. "**Helical microtubules of graphitic carbon"**. Nature 1991; 354:56–8.

[6] E T Thostenson, Z Ren, and T W Chou. "**Advances in the science and technology of carbon nanotube and their composites: a review**". Compos Sci Technol 2001; 61:1899–912.

[7] "**Radushkevich-Lukyanovich"** .(1952).**http://carbon.phys.msu.ru/publications/1952-radushkevich-lukyanovich.pdf.** (Accessed 02/06/2008.)

[8] J P Salvetat, J M Bonard, N H Thomson, A J Kulik, L Forro, W Benoit, et al. "**Mechanical properties of carbon nanotubes".** Appl Phys A: Mater Sci Process 1999; 68:287–92.

[9] E Herna´ndez, C Goze, P Bernier, and A Rubio. "**Elastic properties of single-wall nanotubes"**. Appl Phys A: Mater Sci Process 1999; 69:255–60.

[10] Collins, G Philip, and P Avouris. "**Nanotubes for Electronics**". Sci American December 2000; 67, 68, and 69.

[11] X Xu, and M M Thwe. "**Mechanical properties and interfacial characteristics of carbon-nanotube-reinforced epoxy thin films".** Appl Phys Lett 2002; 81(15):2833–5.

[12] A Allaoui, S Bai , HM Cheng, and J B Bai. "**Mechanical and electrical properties of a MWNT/epoxy composite"**. Compos Sci Technol 2002; 62:1993–8.

[13] D Qian , E C Dickey, R Andrews , and T Rantel . **"Load transfer and deformation mechanisms in carbon nanotube-polystyrene composites".** Appl Phys Lett 2000; 76(20):2868–70.

[14] P Watts and W K Hsu. **"Behaviors of embedded carbon nanotubes during film cracking".** Nanotechnology 2003; 14:L7–L10.

[15] G Yamamoto, M Omori, and T Hashida and H Kimura. **"A novel structure for carbon nanotube reinforced alumina composites with improved mechanical properties".** Nanotchnology 2008; 19:31707-31714

[16] Meo and M Rossi. "**Prediction of Young's modulus of single wall carbon nanotubes by molecular-mechanics based finite element modelling** ". Compos Sci Technol 66:1597-1605.

[17] S B Meo and R Andrews. "**Carbon Nanotubes: Synthesis, Properties, and Applications**". Crit. Rev. Solid State Mater. Sci. 26(3):145-249

[18] **"Carbon nanotube".**http://upload.wikimedia.org/wikipedia/commons/3/35/CNT names.png. (Accessed 08/14/2008).

[19] Dekker and Cees "**Carbon nanotubes as molecular quantum wires**". Phys Today May 1999 ; 52 (5): 22 - 28. Retrieved on **2007-07-28**

[20] T Erik. Thostenson, Z Ren, and T Chou. **"Advances in the science and technology of carbon nanotubes and their composites: a review".** Compos Sci Technol 2001; 61: 1899–1912.

[21] C Journet, W K Maser, P Bernier, A Loiseau, de la M L Chapelle, S Lefrant, et al. **"Large-scale production of single-walled carbonnanotubes by the electric-arc technique".** Nature 1997; 388:756–8.

[22] H W Kroto, J R Heath, S C O'Brien, R F Curl, and R E Smalley. **"C60: Buckminsterfullerene"**. Nature 1985; 318:162–3.

[23] A G Rinzler, J Liu, H Dai, P Nikolaev, C B Huffman, FJ Rodriguez- Macias et al. **"Large-scale purification of single-wall carbon nanotubes: Process, product and characterization".** Appl Phys A 1998;67(1):29–37.

[24] P Nikolaev, M J Bronikowski, R K Bradley, F Fohmund, DT Colbert, KA Smith et al. **"Gas-phase catalytic growth of single-walled carbon nanotubes from carbon monoxide".** Chem Phys Lett 1999;313(1-2):91–7.

[25] S Iijima, T Ichlhashi. **"Single-shell carbon nanotubes of 1-nm diameter".** Nature 1993; 363:603–5.

[26] D S Bethune, C H Kiang, M S Devries, G Gorman, R Savoy, J Vazquez, et al. **"Cobalt-catalyzed growth of carbon nanotubes with single-atomic-layer walls"**. Nature 1993; 363:605–7.

[27] M B Nardelli, B I Yakobson, and J Bernholc. **"Brittle and ductile behavior in carbon nanotubes"**. Phys Review Lett 1998; 81(21):4656–9.

[28] Z Shi, Y Lian, F H Liao, X Zhou, Z Gu, Y Zhang et al. **"Large scale synthesis of single-wall carbon nanotubes by arc discharge method"**. Phys Chem Sol 2000; 61(7): 1031.

[29] Y Saito, K Nishikubo, K Kawabata, and T Matsumoto. **"Carbon nanocapsules and single-layered nanotubes produced with platinum- group metals (Ru, Rh, Pd, Os, Ir, Pt) by arc discharge"**. Appl Phys 1996; 80(5):3062–7.

[30] A Thess, R Lee, P Nikolaev, H J Dai, P Petit, J Robert, et al. **"Crystalline ropes of metallic carbon nanotubes"**. Appl Sci 1996; 273: 483–7.

[31] G M Odegard, T S Gates, K E Wise, C Parka, and E J Siochi. "**Constitutive modeling of nanotube–reinforced polymer composites"**. Compos Sci Technol 2003; 63: 1671–1687.

[32] A K Rappe and C J Casewit. **"Molecular mechanics across chemistry".** Sausalito (CA): University Science Books; 1997.

[33] M P Allen, and D J Tildesley." **Computer simulation of liquids".** Oxford: Oxford University Press; 1987.

[34] D C Rapaport. **"The art of molecular dynamics simulation".** Cambridge: Cambridge University Press; 1995.

[35] D Frankel and B Smit. **"Understanding molecular simulation: from algorithms to applications"**. San Diego: Academic Press; 199

[36] E M Duffy, P J Kowalczyk, and W L Jorgensen. **"Do denaturants interact with aromatic hydrocarbons in water".** Amer Chem Soc 1993; 115:9271–5.

[37] W L Jorgensen, J D Madura, and C J Swenson. **"Optimized intermolecular potential functions for liquid hydrocarbons"**. Amer Chem Soc 1984; 106:6638–4

[38] W L Jorgensen and D L Severance. **"Aromatic–aromatic interactions: free energy profiles for the benzene dimer in water, chloroform, and liquid benzene".** Amer Chem Soc 1990; 112:4768–74.

[39] S Vaknin. **"The Quantum of Continuity"**. http://samvak.tripod.com/cont.html. (Accessed 06/12/2008).

[40] M Monthioux, B W Smith, B Burteaux, A Claye, J Fisher, and D E Luzzi. **"Sensitivity of single-wall nanotubes to chemical** processing: An electron microscopy investigation", Carbon 39 (2001) 1261–1272

[41] **"Dynamic Analysis of Tall Building Using Reduced-Order Continuum Model"**.http://scitation.aip.org/getabs/servlet/GetabsServlet?prog=normal&id=JSENDH000122000011001284000001&idtype=cvips&gifs=yes.(Date Accessed 08/10/2008).

[42] C A Cooper, S R Cohen, A H Barber, and H D Wagner. **"Detachment of carbon nanotubes from a polymer matrix."** Appl Phys Lett 2002; 81:3873–5.

[43] A H Barber, S R Cohen, and H D Wagner. **"Measurement of carbon nanotube-polymer interfacial strength"**. App Phys Lett 2003; 82: 4140–2.

[44] S J Frankland, A Caglar, D W Brenner, and M Griebel. **"Molecular simulation of the influence of chemical cross-links on the shear strength of carbon nanotube-polymer interfaces".** Phys Chem B 2002; 106:3046–8..

[45] K L Lu, M Lago, Y K Chen, M L Green, P J Harris, and S C Tsang. **"Mechanical damage of carbon nanotubes by ultrasound"**. Carbon 1996;34:814.

[46] K B Shelimov, R O Esenaliev, A G Rinzler, C B Huffman, and R E Smalley. **"Purification of single-wall carbon nanotubes by ultrasonically assisted filtration"**. Chem Phys Lett 1998;282:429– 34.

[47] M Zhang, M Yudasaka, A Koshio, and S Iijima. **"Effect of polymer and solvent on purification and cutting of single-wall carbon nanotubes".** Chem Phys Lett 2001; 349:25–30.

[48] A Yasmin, J L Abot, and I M Daniel. **"Processing of clay/ epoxy nanocomposites by shear mixing"**. Scr Mater 2003; 49: 81.

[49] F Robl. 1970**. "Development and application of a continuum theory of mixtures including electromagnetic and thermodynamic aspects".** http://worldcat.org/oclc/26993020**.** (Accessed 12/8/2008).

[50] B S Altan, I Miskioglu, and C R Vilmann. **“Propagation of s-h waves in laminated composites: a gradient elasticity approach ”.** J Vib and Cont, Vol. 9, No. 11, 1265-1283. (2003)

[51] S Elangovan, B S Altan, and G M Odegard. **“An elastic micropolar mixture theory for predicting elastic properties of cellular materials”.** Mech Mat Vol 40, Issue 7, Pages 602-615. July 2008.

[52] C Radin. 1986. **“Crystals and quasicrystals: a continuum model”. http://ProjectEuclid.org/getRecord?id=euclid.cmp/1104115430.** (Accessed 12/8/2008).

[53] J Dong. 1993. **“A continuum mixture theory of wave propagation in axially polarized piezoelectric fibrous composites”.** http://en.scientificcommons.org/jennifer_jingxuan_dong. (Accessed 12/8/2008).

[54] Ingram, J D Eringen, and A Cemal. 2005 **“Continuum theory of chemically reactinglmedia”.**http://en.scientificcommons.org/repository/defense_technical_information_center_oai-pmh_repository. (Accessed 12/8/2008).

[55] A H Nayfeh and W G Abdelrahman. “**An improved continuum mixture model for wave propagation in fibrous composites**”. Acoust Soc of Amer, Vol 104, No 2, Pages 867-73. August 1998.

[56] Monthioux, Marc, Kuznetsov, and L Vladimir. (2006). "**Who should be given the credit for the discovery of carbon nanotubes?**". Carbon 44. doi:10.1016/j.carbon.200 03.019. Retrieved on 2007-07-26.

[57] Q Wanga. **"Wave propagation in carbon nanotubes via nonlocal continuum mechanics"**.Appl Phys 98, 124301 (2005).

[58] G A Antonelli, H J Maris, Malhotra, and Harper,**"picosecond ultrasonics study of thevibrational modes of a nanostructure"**. Appl Phys 91, pp 3261-3267

[59] J Yoon, C Q Ru, and A Moiduchowski, **"Sound wave propagation in multiwall carbon nanotubes",** 93 (2003), pp. 4801-4806

[60] T Natsuki, T Hayashi, and T Endo. **"Wave propagation of carbon nanotubes embedded in an elastic medium"**. Appl Phys 97,044307.

[61] Y Zhang and S Iijima. **"Formation of single-wall carbon nanotubes by laser ablation of fullerenes at low temperatures".** Appl Phys Lett 1999;75(20):3087–9.

[62] H Rajoria and N Jalili. **"Passive vibration damping enhancement using carbon nanotube-epoxy reinforced composites".** Compos Sci Technol 2005; 2079-2093.

[63] J Sandler, M S Shaffer, T Prasse, W Bauhofer, K Schulte, and A H Windle. **"Development of a dispersion process for carbon nanotubes in an epoxy matrix and the resulting electrical properties"**. Polymer 1999; 40:5967–71.

[64] A Allaoui, S Bai, H M Cheng, and J B Bai. **"Mechanical and electrical properties of a MWNT/epoxy composite"**. Compos Sci Technol 2002; 62:1993–8.

[65] Z Ounaies, C Park, K E Wise, E J Siochi, and J S Harrison. **"Electrical properties of single wall carbon nanotube reinforced polyimide composites".** Compos Sci Technol 2003;63: 1637–4

[66] E T Thostenson, and T W Chou. **"On the elastic properties of carbon nanotube-based composites: modeling and characterization"**. J Phys D: Appl Phys 2003; 36:573–82.

[67] A H Nayfeh. "**Wave Propagation in Layered Anisotropic Media with Application to Composites**". Elsevier, Amsterdam, 1995.

VITA

Elaf Naeem Shaker Mahrous, was born in **Jeddah-KSA** in **1984**, he has got his **Bachelor of Science degree** in **Mechanical Engineering** in **2006** from **King Fahad University of Petroleum and Miner**als in **KSA**. He followed it by the **Master of Science** degree also in **Mechanical Engineering** in the field of the nano-technology and carbon nano-tube composites from **King Fahad University of Petroleum and Minerals** in **2009**. During his MS thesis he worked as a process engineer, rotating equipment engineer, and maintenance engineer in Saudi Aramo Company, and he worked also as a sales engineer in EagleBurgmann Company. His Area of Interest includes the development of the carbon nano-tubes composites analysis models.